Collaborative Research: Adaptive Responses of **Phaeocystis** *populations in Antarctic ecosystems (Phantastic)*

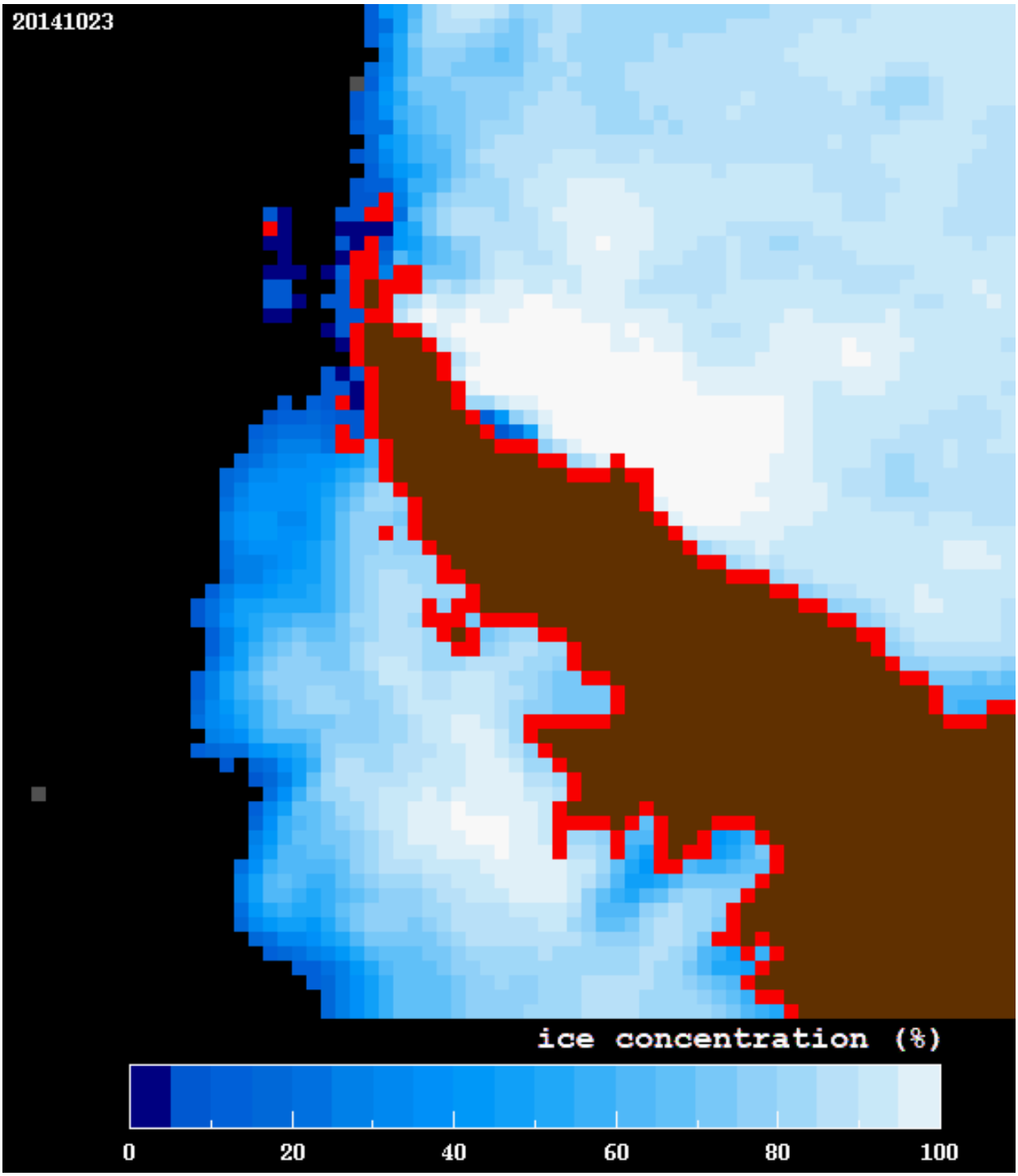

Table of Contents

Collaborative Research: Adaptive Responses of *Phaeocystis* populations in Antarctic ecosystems (Phantastic)

Introduction

The haptophyte algal genus *Phaeocystis* is a key component of the phytoplankton community in highly productive waters over much of the globe, with *Phaeocystis antarctica* (Figure 1) dominating in the Southern Ocean (Schoemann et al 2005). This species is critical to Southern Ocean ecology and biogeochemistry because it is both an integral part of the sea ice community and it forms massive water column blooms (chlorophyll *a* >10 mg m^{-3}) that contribute significantly to CO_2 drawdown and subsequent carbon (C) export below the euphotic zone (Smith and Gordon 1997, Asper and Smith 1999, DiTullio et al. 2000, Arrigo et al. 2003 2008). Phytoplankton productivity in the Southern Ocean is usually limited by the availability of iron (Fe), leaving high concentrations of nitrate, phosphate and silicate that are not utilized (Boyd et al 2007 and references therein).

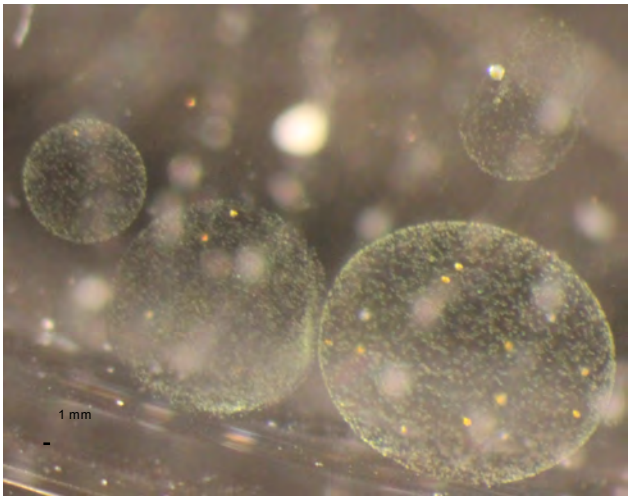

Fig. 1. *Phaeocystis antarctica* colonies from the Amundsen Sea.

Understanding the factors controlling the distribution of *P. antarctica* within the Southern Ocean is important because this taxon differs considerably from other phytoplankton types (e.g. diatoms) in terms of its biogeochemistry and its functional role within Southern Ocean ecosystems. For example, *P. antarctica* has an unusually low requirement for phosphorus (P) relative to C (Arrigo et al. 1999, 2002), particularly for a bloom forming algal species (Klausmeier et al. 2004). As a result, it is very efficient at lowering surface water CO_2 concentrations and facilitating enhanced air-sea exchange (Arrigo et al. 2008). *P. antarctica* also has the ability to form large (1 mm) colonies (Schoemann et al. 2005), a strategy that may provide additional storage capacity for metabolically active compounds as well as enable it to more effectively resist grazing. Because it is not heavily grazed, it forms the base of a marine food web that is substantially different from that supported by diatoms (Tagliabue and Arrigo 2003) and is an efficient vehicle for exporting particulate C to the deep ocean (DiTullio et al. 2000). Finally, *P. antarctica* produces large amounts of dimethylsulfoniopropionate, making it a potentially important component of the global sulfur cycle (DiTullio and Smith 1995).

Objective of Phantastic

Our objective is to use a combination of field- and laboratory-based studies to identify the environmental factors (in addition to light) that control the distribution of *P. antarctica* in the Southern Ocean and to identify the specific adaptive responses to these environmental factors. The field program will include cruises to both the Ross Sea and west Antarctic Peninsula (wAP) to sample both the waters of the open ocean and the major coastal polynyas in each region where *P. antarctica* is found, albeit to varying degrees, and where environmental conditions vary widely. The Ross Sea contains both the Terra Nova Bay and the Ross Sea polynyas, only the latter of which supports large *P. antarctica* populations. The wAP is home to modest populations of *P. antarctica*, although the conditions under which it grows differs markedly from

that in the Ros Sea. ***By assessing the factors that control the growth of* P. antarctica *in these different, we will better understand the physiological and genetic adaptations that control its spatial distribution.***

Specifically, we will investigate genome-wide differences in *P. antarctica* gene expression and link these to physiological performance of *P. antarctica* during the evolution of the bloom. We will characterize genetic diversity of *P. antarctica* populations in the Ross and Amundsen Seas and the open ocean. By merging oceanographic, geochemical, and physiological studies with a host of genome technologies, we will dissect the conditions that provoke gene expression and acclimation responses in *P. antarctica* populations that have high growth rates, resist grazing by zooplankton, and have the capacity to survive marked seasonal changes in their environment. These studies will strongly impact our basic understanding of the physiology and ecology of *P. antarctica* and acclimation processes that control its success in the Southern Ocean.

The participants on the Phantastic II cruise were:

Name	**Participant Description**	**University**
Kevin R. Arrigo	Scientist, Chief	Stanford University
Anne-Carlijn Alderkamp	Scientist	Stanford University
Gerrit L. van Dijken	Scientist	Stanford University
Kate E. Lowry	Graduate student	Stanford University
Kate M. Lewis	Graduate student	Stanford University
Hannah Joy- Warren	Graduate student	Stanford University
Virginia Selz	Graduate student	Stanford University
John Butterfield	Graduate student	Stanford University
Alessandra Santiago	Graduate student	Stanford University
Caroline Ferguson	Graduate student	Stanford University
Erin Dillon	Undergraduate student	Stanford University
Yussi Delgado	Graduate student	Monash University, Australia
Tom Delmont	Scientist, Post-Doc	Marine Biological Laboratory
Laura Z. Filliger	Graduate student	University of Rhode Island
Erin MarieBertrand	Postdoctoral Research Fellow	J. Craig Venter Institute
Hilde Oliver	Graduate student	University of Georgia
Rob Middag	Scientist	University of Otago, New Zealand
Ella Rose Patterson	Graduate student	University of Otago, New Zealand
Janice Nash-Arrigo	Elementary school teacher	Addison Elementary School
Zachary Erickson	Graduate student	California Institute Technology

The Phantastic II cruise description

Kevin Arrigo, Anne-Carlijn Alderkamp, Zachary Erickson

During Phantastic II, we collected biological and biogeochemical data across five hydrographic transects comprising 100 water column stations along the wAP between 31 October and 21 November 2014 (Figure 2). These transects coincide with those sampled during the Palmer LTER, although each transect was 400 km long during Phantastic II (200 km for Palmer LTER). A segment along the shelf break (roughly corresponding to the 650 m isobath) between LTER lines 200 and 300 was also sampled. Regular station spacing was 25 km, although this was reduced when crossing the continental shelf break on lines 200, 300, 600, and 700

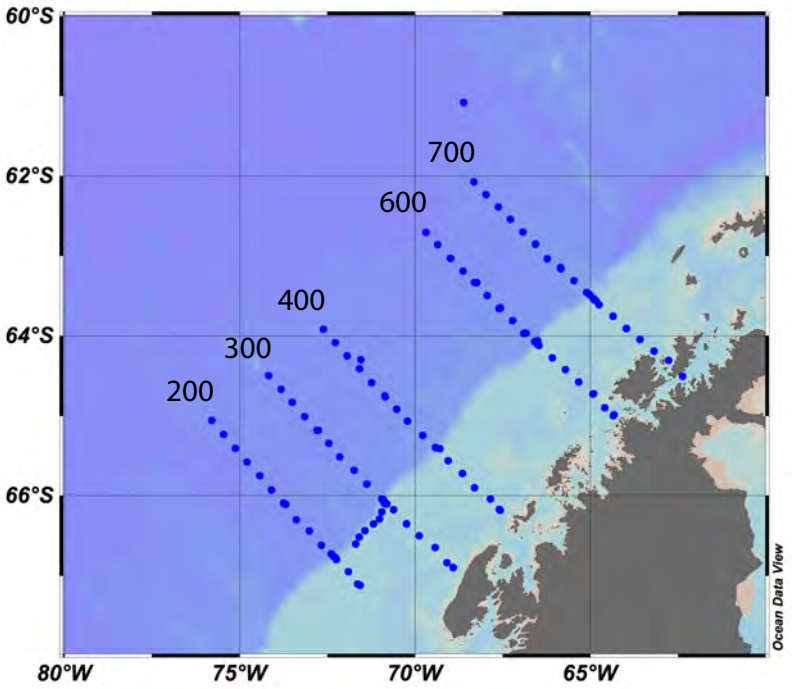

Fig. 2. Hydrographic stations sampled during Phantastic II.

Hydrography. Two CTD instruments were used during the cruise: a "Conventional" CTD (Conv) and a trace-metal clean CTD (TMC). On November 5, during station 36, cast 2, the cable holding the rosette broke and we lost the TMC. After this catastrophe, we were able to use two spare GO-FLO bottles to sample for trace metals – these casts are abbreviated TMW (trace-metal wire). Occasionally, samples were taken of surface water from a Zodiac (Zod). Four types of stations were sampled: Full daily stations (all measurements, samples for experiments), main stations (most measurements, samples for experiments), chlorophyll-only stations (only conventional CTD and limited measurements), and sensor-only stations (only conventional CTD, only taking water samples for specific reasons, generally taken over the shelf break). These are summarized in Table 1.

Sensors deployed with the CTD-rosette package included a fluorometer (WET Labs ECO-AFL/FL), a transmissometer (WET Labs C-Star), and an oxygen sensor (SBE-43) for all casts as well as a PAR/Irradiance sensor (Biospherical/Licor) for casts shallower than 1000 m. Using the conventional CTD rosette, we collected water at discrete standard depths in the upper water column for measurements of phytoplankton pigment and elemental composition via filtrations, variable chlorophyll *a* fluorescence, and community composition. Additionally, we collected nutrient samples at the standard depths described above plus deeper depths (e.g. 150 m, 200 m, 300 m, 400 m, 500 m, and 750 m). At shelf stations with bottom depth <750 m, we collected seawater at 10 m and 20 m above the seafloor. Station locations are illustrated below, with station spacing of ~25 km along the five transects (corresponding to the Palmer LTER grid lines 200, 300, 400, 600, and 700).

The typical CTD cast procedure was as follows. The CTD was lowered into the water to allow the sensors to equilibrate at ~10 m depth. The sensors were considered equilibrated when

all duplicate sensors agreed well with each other, which generally took about one minute. Then the CTD was raised to 2 m depth before being lowered to the maximum depth. The maximum speed of descent was ~60 m/min, and varied depending on conditions. No bottles were fired during the down-cast. Instead, the operator would watch the sensor profiles to plan where the bottles would be triggered on the up-cast. The desired depths for most measurements (the "core" depths) were 2, 10, 25, 50, 75, and 100 m. If a fluorescence maximum existed at another depth, either the closest bottle would be moved to that depth, or the 75 m bottle would be moved to that depth. Note that a fluorescence maximum was generally only considered valid if there also existed a transmission minimum at the same depth.

The standard depths for nutrient profiles were the core depths as well as 150, 200, 300, 400, 500, and 750 m. If the ocean depth was <750 m, the bottom depth was also sampled (here, "bottom" means ~10 m above sea floor, as it was considered unwise to bring the CTD much closer than that), as well as occasionally "bottom – 10 m", and the other bottle depths were modified to give a complete profile.

These bottle depths were designed to be somewhat fluid, and were able to be moved by up to ~10 meters to capture interesting features observed on the down-cast or to avoid triggering a bottle on a steep gradient. In practice, the standard depths (2, 10, 25, 50, 75, 100, 150, 200, 300, 400, 500, and 750 m) were generally used "as is".

Generally, the CTD would stop at the chosen depth and wait for ~30 seconds before closing the bottle. The rosette displaces water during the upcast, and it is generally understood that ocean water is in effect "dragged upward" by the rosette, meaning during the up-cast the CTD sensors are "contaminated" by water being swept along in the CTD's wake. This waiting time allows the water caught in the updraft to dissipate, so that the CTD sensors are measuring the correct water mass. Sometimes, at the discretion of the ET (electronics technician) operator and due to ship movement, this waiting period was omitted. After the bottle was fired, the CTD would be raised to the next bottle depth.

CTD data processing. Data from the CTD casts were processed by SeaBird software by technicians onboard the NBP and binned by depth (1 m bins) into .cnv files located in the /data/ocean/ctd/process folder. Also present in this folder are files with information on the CTD rosettes (.ros) and the sensor readings at the locations where bottles were triggered (.btl). The file format for all of these is "nbp1409SSS_CC.ext", where "SSS" is the three-digit station number, "CC" is the two_digit cast number, and "ext" is the extension. Files from the TMC are named as "nbp1409trSSS_CC.ext". Down (up)-cast binned data have "d" ("u") appended to the filename before the extension; *i.e*. nbp1409007_01d.cnv.

Four data files are created during each cast, and stored in the folder /data/ocean/ctd/raw. The extension .xmlcon is a configuration file, .hdr is a header file containing useful information about each cast, .hex is the raw data, and .bl is a file which records information about when bottles are fired. This last file contains five comma-delimited columns. The first three columns contain information on the number of the bottle fired, its position in the rosette, and the time. The fourth and fifth column contain the minimum scan number and the maximum scan number, which SeaBird software uses to determine which scans to average when it computes the sensor information for each bottle. Our understanding of the software protocol is that the minimum scan number is the scan at which the bottle is fired, and the maximum scan number is the scan 1.5 seconds later. This means that all .btl files processed routinely on the NBP recorded averaged data starting when the bottle was closed and ending 1.5 seconds later, when the sensor was already moving upwards through the water column. Therefore, it might be useful to re-process these .btl files to use data from 1.5 - 0 seconds *before* the bottle was closed.

To re-process the data using SeaBird software, first download the SBEDataProc.exe executable from http://www.seabird.com/software/sbe-data-processing. Running this program

and using the steps below in the order given will give files virtually identical to that found in the .btl and .cnv files in the /data/ocean/ctd/process folder, except the .btl files will provide information on the averaged values in the timeframe 1.5 – 0 seconds *before* the bottle was fired, and the oxygen data will be in units of µmol/kg. Note that the steps below are designed to give you information in as close a format as the data processed on board the NBP as possible; depending on which variables you are interested in, the process could be slightly different. For help and more information, download the SBE Data Processing Manual at: http://www.seabird.com/document/sbe-data-processing-manual.

Transect plots. Interpolated potential density, potential temperature, and salinity data from each transect are shown in Figures 3-6. Data were taken from the .cnv files processed on board the NBP (downcast only) and stored in /data/oceans/ctd/process. All other processing was done using MATLAB 2014b. For each station, the deepest cast was used (conventional or TMC); these depths are indicated by light grey lines. Station data were interpolated in the horizontal dimension using the 'pchip' routine. The code is provided in the MATLAB script make_ctdplots.m. Bathymetry was taken from the IBCSO (International Bathymetric Chart of the Southern Ocean) V1.0 dataset in polar stereographic with true scale at 65° referenced to WGS84 ellipsoid and 500 m resolution, downloadable in netCDF format as .grd files from http://doi.pangaea.de/10.1594/PANGAEA.805734?format=html (download both the bedrock elevation and the source identification grid).

A few stations were not processed in making these datasets. In transect 600, station 12 was not included because it lies a considerable distance off of the transect line due to ship drift. In transects 700 and 300, stations 34 and 66 were not included because they were temporally quite distinct from the adjacent stations.

Figure 3: Transect 700

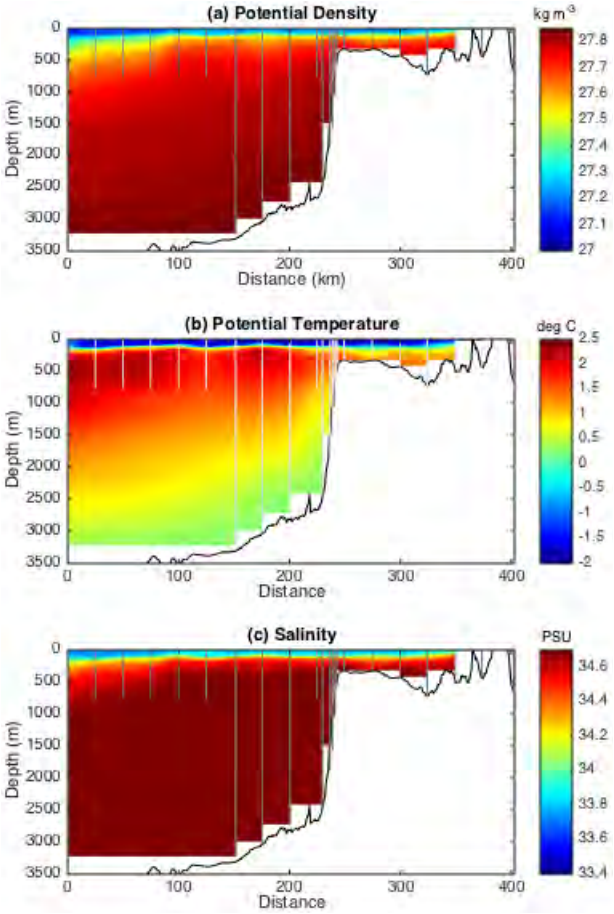

Figure 4: Transect 600

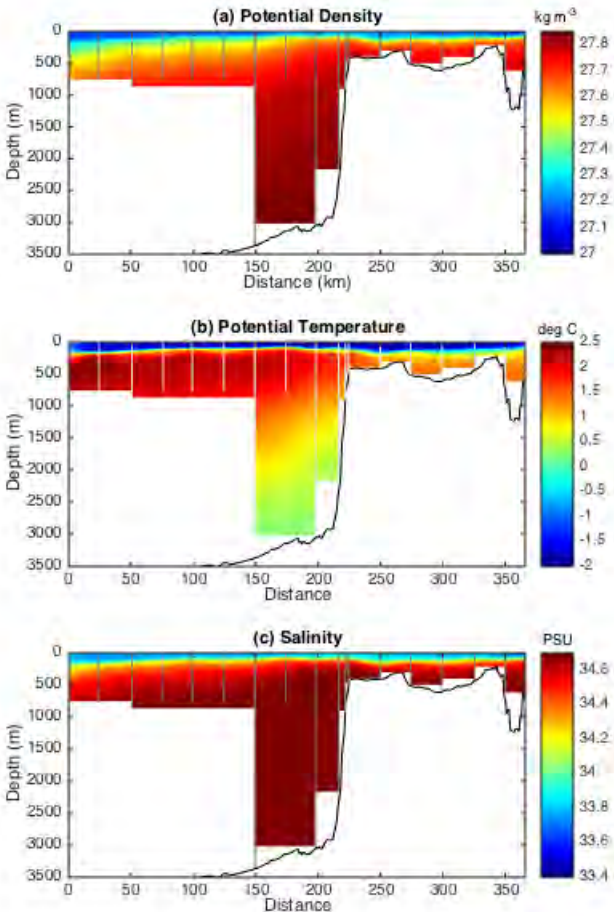

Figure 5: Transect 400

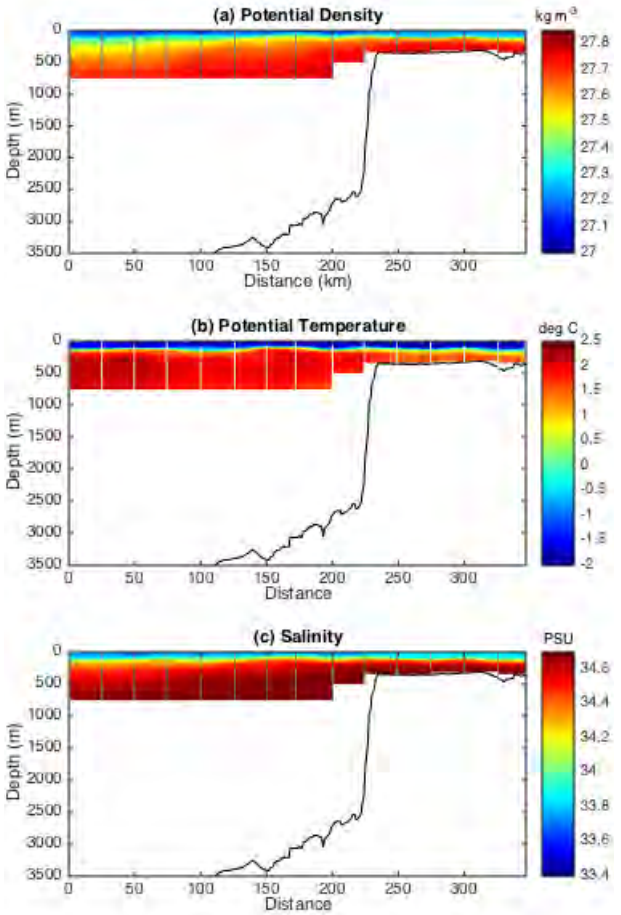

Figure 6: Transect 300

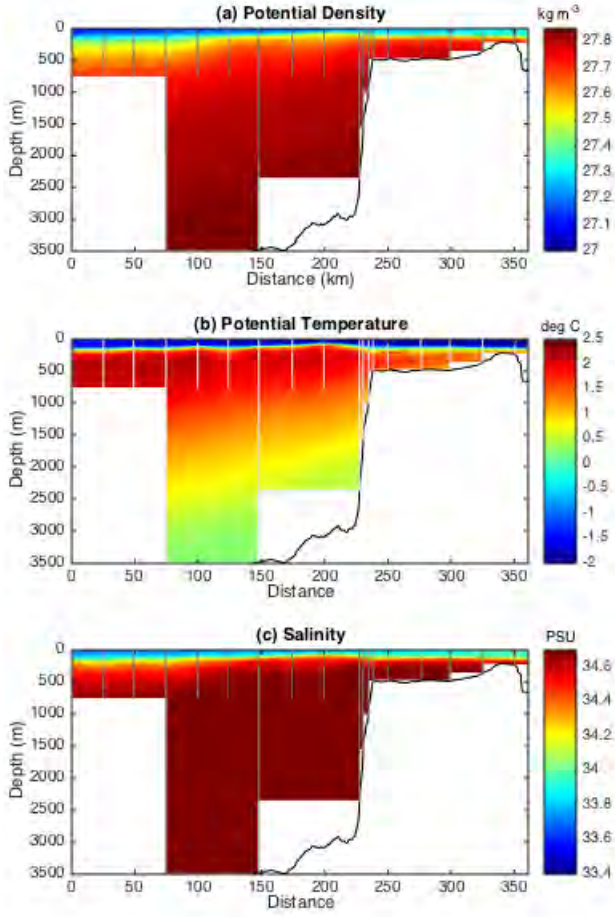

Table 1: Lists all stations along with the CTD types associated with each and the LTER transect. Type key: FD = full daily station, M = main station, C = chlorophyll-only station, S = sensor-only station.

Station	Type	Day	Lat.	Long.	CTD Types	Transect	Station	Type	Day	Lat.	Long.	CTD Types	Transect
1	Test	10/30	-61.08	-68.61	Conv, TMC	NA	51	C		-66.26	-73.42	Conv	200
2	M	10/31	-62.70	-69.69	Conv, TMC	600	52	M	11/10	-66.44	-73.02	Conv, TMW	
3	C		-62.86	-69.35	Conv		53	C		-66.62	-72.67	Conv	
4	FD		-63.03	-68.99	Conv, TMC		54	FD		-66.77	-72.27	Conv, TMW	
5	C		-63.19	-68.64	Conv		55	S		-66.80	-72.24	Conv, TMW	
6	M		-63.33	-68.30	Conv, TMC		56	S	11/11	-66.73	-72.39	Conv	
7	C		-63.50	-67.95	Conv		57	S		-66.76	-72.33	Conv	
8	M	11/01	-63.65	-67.57	Conv, TMC		58	FD		-66.94	-71.92	Conv, TMW	
9	C		-63.78	-67.24	Conv		59	M		-67.12	-71.58	Conv, TMW	
10	FD		-63.97	-66.87	Conv, TMC		60	C	11/12	-66.60	-71.69	Conv	Shelf break
11	S		-64.07	-66.59	Conv		61	C		-66.52	-71.59	Conv	
12	S		-64.06	-66.54	TMC		62	C		-66.44	-71.44	Conv	
13	S	11/02	-64.10	-66.52	Conv		63	M		-66.34	-71.19	Conv, TMW	
14	S		-64.13	-66.45	Conv		64	C	11/13	-66.29	-71.02	Conv	
15	C		-	-	Conv		65	C		-	-	Conv	

			64.27	66.10						66.20	70.96		
16	FD		-64.42	-65.71	Conv, TMC		66	FD		-66.10	-70.85	Conv, TMW	300
17	C		-64.57	-65.34	Conv		67	M		-66.17	-70.62	Conv, TMW	
18	M		-64.72	-64.91	Conv, TMC		68	FD	11/14	-66.35	-70.24	Conv, TMW	
19	C		-64.90	-64.58	Conv		69	C		-66.50	-69.88	Conv	
20	M		-64.99	-64.33	Conc, TMC		70	M		-66.65	-69.42	Conv, TMW	
21	FD	11/03	-64.50	-62.37	Conv, TMC	700	71	FD	11/15	-66.84	-69.09	Conv, TMW	
22	C		-64.31	-62.77	Conv		72	C		-66.90	-68.91	Conv	
23	M		-64.19	-63.19	Conv, TMC		73	FD	11/16	-66.18	-67.57	Conv, TMW	400
24	C		-64.05	-63.57	Conv		74	C		-66.04	-67.85	Conv	
25	M	11/04	-63.91	-63.96	Conv, TMC		75	M		-65.90	-68.31	Conv, TMW	
26	C		-63.76	-64.32	Conv		76	C	11/17	-65.72	-68.65	Conv	
27	FD		-63.61	-64.75	Conv, TMC		77	M		-65.57	-69.08	Conv, TMW	
28	S		-63.56	-64.84	Conv		78	FD		-65.40	-69.35	Conv, TMW	
29	S		-63.55	-64.86	Conv		79	C		-65.24	-69.78	Conv	
30	S		-63.54	-64.89	Conv		80	M	11/18	-65.10	-70.12	Conv, TMW	
31	S		-63.5	-64.9	Conv		81	C		-64.9	-70.5	Conv	

			3	2						2	2		
32	S		-63.48	-65.03	Conv		82	FD		-64.76	-70.86	Conv, TMW	
33	C		-63.45	-65.01	Conv		83	C		-64.59	-71.24	Conv	
34	S		-63.54	-64.90	TMC		84	M		-64.35	-71.56	Conv, TMW	
35	C	11/05	-63.31	-65.45	Conv		85	C	11/19	-64.25	-71.91	Conv	
36	FD		-63.15	-65.85	Conv, TMC		86	M		-64.10	-72.25	Conv, TMW	
37	C		-63.04	-66.23	Conv		87	C		-63.92	-72.62	Conv	
38	M	11/06	-62.85	-66.57	Conv, Zod.		88	FD		-64.49	-74.18	Conv, TMW	300
39	C		-62.71	-66.92	Conv		89	C		-64.67	-73.83	Conv	
40	M		-62.54	-67.28	Conv		90	M		-64.83	-73.51	Conv, TMW	
41	C		-62.39	-67.61	Conv		91	C	11/20	-65.01	-73.16	Conv	
42	FD		-62.23	-67.97	Conv, Zod.		92	M		-65.17	-72.81	Conv, TMW	
43	C		-62.07	-68.32	Conv, Zod.		93	C		-65.31	-72.50	Conv	
44	M	11/08	-65.05	-75.59	Conv, TMW	200	94	M		-65.52	-72.12	Conv, TMW	
45	C		-65.23	-75.47	Conv		95	C	11/21	-65.67	-71.75	Conv	
46	FD		-65.41	-75.13	Conv, TMW		96	M		-65.82	-71.45	Conv, TMW	
47	C		-65.58	-74.79	Conv		97	S		-66.04	-70.95	Conv	

48	M		-65.75	-74.44	Conv		98	S		-66.05	-70.90	Conv	
49	C	11/09	-65.93	-74.10	Conv		99	S		-66.09	-70.89	Conv	
50	FD		-66.10	-73.75	Conv, TMW		100	S		-66.10	-70.81	Conv	

Nutrients, Phytoplankton, and Remote Sensing

Kevin R. Arrigo, Anne-Carlijn Alderkamp, Gert van Dijken

Nutrients

Samples for dissolved nutrient concentrations (nitrate, nitrate, phosphate, and silicate) were taken at every station at every discrete depth sampled with the CTD-rosette package as well as the TMC wire (see subsequent section on Trace Metal Clean sampling). Samples were collected by filtering seawater through a 0.2 μm syringe filter and were frozen at -20˚C for nitrate, nitrate, and phosphate and at +4˚C in the dark for silicate to prevent precipitation. Post-cruise nutrient sample analysis will take place at NIOZ.

Phytoplankton

Phytoplankton samples collected via filtration include chlorophyll *a* concentrations (Chl *a*), phytoplankton pigments through high performance liquid chromatography (HPLC), particulate organic carbon and nitrogen (POC/PON), particulate organic phosphorous (POP), and light absorption by phytoplankton (Ap/Ad). While Chl *a* concentrations were measured at every station, all other filtrations were made at "main" stations spaced ~50 km apart (i.e. every other station). Samples for Chl *a*, HPLC, and POC/PON were taken at all depths in the upper 100 m, while samples for POP and Ap/Ad were taken at two depths per station (typically 10 m and 50 m or the chlorophyll *a* maximum, corresponding to the depths of the PvE curves). To collect phytoplankton samples, seawater was filtered under low vacuum pressure (<5 mg Hg or <150 psi) onto Whatman glass-fiber filters (GF/Fs) with a diameter of 25 mm and a nominal pore size of 0.7 μm, with filtered seawater used to rinse funnels onto the filters. For POC/PON and POP samples, GF/F filters were combusted at 450˚C for 4 hours prior to use. After filtration, filters designated for Chl *a* measurements were stored in 90% acetone (5 mL) in the dark for 24 hours at +4˚C for pigment extraction prior to shipboard analysis before and after acidification using a Turner Designs fluorometer. Filters for HPLC analysis were folded and wrapped in aluminum foil, immediately frozen in liquid nitrogen, and kept frozen at -80˚C until laboratory analysis after the cruise at NIOZ. Filters for POC/PON and POP were dried in an oven at 60˚C for 24 hours and then stored at room temperature until post-cruise analysis. Ap/Ad filters were

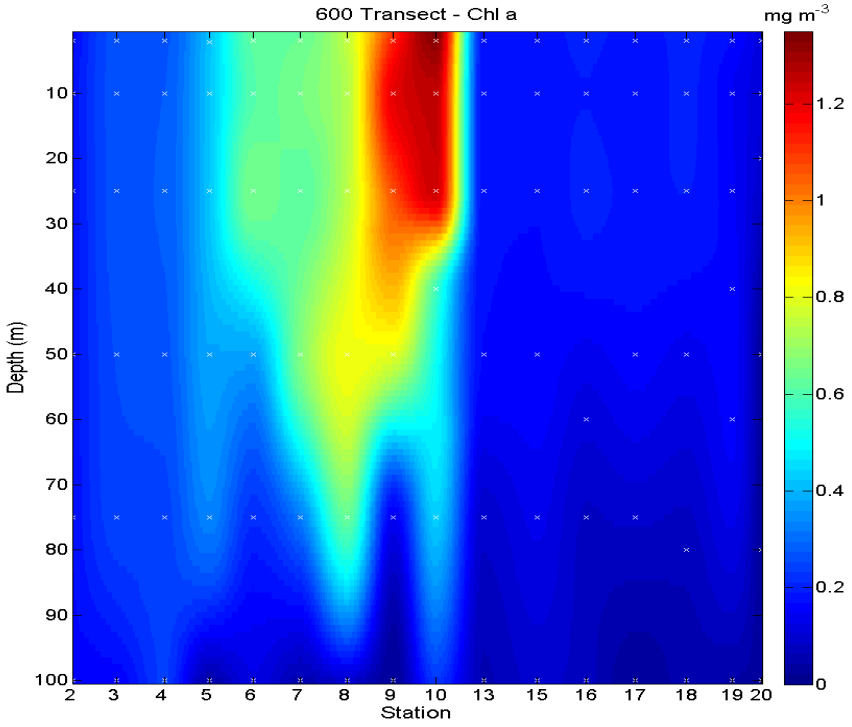

Fig. 1. Vertical section of Chl *a* concentration measured along the 600-line transect.

measured onboard using a Lambda-18 Spectrometer with an integrating sphere, as further detailed with the description of PvE curves.

Phytoplankton variable fluorescence was measured using a FIRe fluorometer (Fluorescence Induction and Relaxation System; Satlantic LP) at every station and a PAM fluorometer (Pulse Amplitude Modulated; Water-PAM, Heinz Walz) at every other station (i.e. "main" stations). Samples were dark acclimated on ice for 30 minutes prior to the determination of the maximum efficiency of photosystem II (Fv/Fm), the functional absorption cross section (σ_{PSII}), and the energy transfer between PSII units.

Phytoplankton community composition was assessed at two depths per station (typically 10 m and 50 m or the chlorophyll *a* maximum, as described above). Samples from stations were imaged at three magnifications (20x, 40x and 100x). Samples imaged with the 2x objective lens (20x magnification) were run using an 800 μm flow cell and were not pre-filtered. Samples imaged with the 4x objective lens were run using a 300 μm flow cell and pre-filtered at 300 μm, and samples imaged with the 10x objective were run on a 200 μm flow cell and pre-filtered at 200 μm. The FlowCAM was focused manually using COUNT-CAL™ Particle Size Standard 50 μm beads (Thermo Scientific). Samples were run until 1000 images were collected or 30 minutes elapsed. The flow cell was flushed with Milli-Q water between samples. When flow cells accumulated stuck particles, the flow cell was filled with a 10% Liquinox solution and sonicated for a couple of minutes. Flow cells were flushed with Milli-Q before using. Additionally, at the location of each FlowCAM sample, water samples were also preserved for cell counts in gluteraldehyde (1 mL in 50 mL seawater for 2% concentration) and stored at +4˚C for post-cruise microscopic analysis.

*P vs E Experiments***.** We studied the characteristics of photosynthesis by natural phytoplankton assemblages at different light levels by performing so-called PvsE curves (photosynthesis vs. irradiance). These were used to determine maximum photosynthetic rates, the light intensity to which phytoplankton is adapted, light limited rates of photosynthesis and photoinhibition parameters. During this cruise a total of 221 PvsE curves were done. They were typically done for two depths at each 'full' station. These depths were normally 10 m (the same depth at which the bio-assay experiments were started) and the depth of the chlorophyll maximum. In addition PvsE curves were done on ice cores and for the bio-assay and ice algae/water column phytoplankton competition experiments.

In short, 13-14 20 mL PET scintillation vials were filled with 2 mL of seawater. Radiolabelled bicarbonate (H14CO3) was added before the vials were transferred into a photosynthetron where they were incubated for 2 hours at 0°C under different light conditions, ranging from 2 to >600 μEin m2 s-1. After incubation, 100 μL of 6 N hydrochloric acid was added and the vials were gently shaken for around 24 hours to drive off inorganic carbon. After neutralization with 100 μL 6N sodium hydroxide, 10 mL of scintiallation cocktail (Ecolume) was added. The samples were then counted for 5 minutes on a liquid scintillation counter.

For each PvsE curve phytoplankton was filtered onto a GF/F filter to generate an absorption spectrum (Ap) of phytoplankton pigments on a Perkin Elmer UV/VIS Lambda 18 spectrophotometer with an integrating sphere from 300-800 nm. This spectrum will be used to quantify the amount of light absorbed during the PvsE incubation and subsequently to calculate the quantum yield of photosynthesis. Detrital absorption (Ad) was also measured after extraction of the sample in 80% methanol.

Simulated in situ primary production. In addition to the 'standardized' PvsE experiments simulated in situ production was estimated. During these experiments carbon fixation by natural phytoplankton is measured by incubating samples in an outside incubator for 24 hours under different light levels. With these experiments photosynthesis at different depths in the water

column can be estimated and a daily column integrated primary production rate can be calculated. A total of 19 simulated in situ experiments were performed.

In short, Falcon flasks (250 mL) were filled with 150 mL of seawater sample. After this radiolabelled bicarbonate (H14CO3) was added. In order to simulate light attenuation in the water column the samples were covered with different layers of neutral density screening. The following optical light levels were used: 85% (no screening), 65%, 25%, 10%, 5% and 1%. Care was taken to select the sample from the appropriate Niskin bottle collected closest to the optical depth at which it was incubated. After 24 h incubation time 30 mL of sample was filtered in triplicate over GF/F filters. The filters were acidified with 100 µL of 6N hydrochloric acid to drive off inorganic carbon. After addition of 5 mL of scintillation cocktail (Ecolume) the samples were counted on a liquid scintillation counter.

Satellite Remote Sensing

Ocean color satellite images showing phytoplankton biomass distributions were very helpful during of this cruise. Using these images as a guide, we were able to track areas with high phytoplankton biomass in our quest to sample Phaeocystis dominated waters in the Antarctic Peninsula region.

An automated system was set up at Stanford University to have MODIS/Aqua oceancolor data send to us on the research vessel by email. Through a near real-time data subscription using the NASA Ocean Biology Processing Group's data subscription service satellite scenes were downloaded every 3 hours from NASA ftp-servers. After downloading the files the chlorophyll product was extracted and mapped to a common projection. Daily composites were generated from individual scenes (4-8 per day) as well. In addition ice concentration (National Snow & Ice Data Center (NSIDC)) and sea surface height data (AVISO, aviso.altimetry.fr) for locating eddies and fronts was downloaded and reprojected the same way as the ocean color data. All images were then emailed to us in a compressed kml format (kmz), so it could be easily used with the Google Earth software package. See examples of these images elsewhere in the cruise report.

Trace Metal Work

Rob Middag

Iron (Fe) has been shown to be a limiting nutrient for phytoplankton growth in Antarctic waters (Coale et al., 1996; de Baar et al., 1990; Martin et al., 1994) (, even in the productive continental shelves surrounding the Antarctic continent (Arrigo et al., 2003). The abundance of Fe in seawater is controlled by a balance between Fe input (via sediment resuspension, sea-ice and glacial melt, upwelling, atmospheric deposition, hydrothermal inputs and lateral and vertical diffusion from sources), stabilization processes via organic complexation that keep Fe in the dissolved phase, and by removal processes like (oxidative) precipitation, adsorptive scavenging, and phytoplankton uptake (Alderkamp et al., 2012; Bruland, 2014; Gerringa et al., 2012; Klunder et al., 2012; Thuroczy et al., 2011; Thuroczy et al., 2012).

The composition, sources and provenances of iron binding ligands that keep Fe stable in solution in seawater are still largely unknown. Predictions can be made about how much iron is bioavailable and how much more iron might be stabilised in solution (Maldonado et al., 2005). As Fe in excess of the ligand concentration quickly precipitates(Buck and Bruland, 2007), the ligand concentration gives an upper bound to the maximum amount of Fe that can be supplied and remain in solution. Comparison of ligand saturations and concentrations in the different treatments in the bio-assay experiments will elucidate if the ligand saturation is dependent on light intensity or if ligands are produced during the experiments. Siderophores, small molecules produced by microorganisms to facilitate iron acquisition (Velasquez et al., 2011), would be expected to be produced in iron-limited treatments.

However, the influence of other metals or vitamins on phytoplankton productivity cannot be excluded either (Bertrand et al., 2007; Browning et al., 2014; Middag et al., 2011; Middag et al., 2013). Like trace metals, phytoplankton require access to cobalamin from seawater, where it is produced by bacteria. Importantly, however, the potential role of other metals or cobalamin on primary production and species dominance has not yet been extensively studied

Objectives. For the Phantastic project our objectives are four-fold.

1. Identifying the sources of Fe and other bio-essential metals by:
    a. Measuring DFe shipboard at all stations
    b. Measuring Cd, Co, Cu, Fe, Mn, Ni, Zn, Ti, Y, La, Pb and Ga via ICP-MS (shore based). All stations for dissolved metal, selected stations for total dissolvable metals (unfiltered samples)
    c. Measuring $\delta^{18}O$ to assess glacial and sea ice melt input (shore based) at all stations
    d. Measuring $\delta^{234}U$ and $\delta^{238}U$ to track the release of weathering products and anoxic conditions (shore based) at selected stations
    e. Measuring $\delta^{56}Fe$ to distinguish different Fe sources (shore based) at selected station

2. Qualifying and quantifying the organic speciation of Fe (Fe-binding ligands) at selected stations to know the capacity of the water to keep Fe in solution and identify what ligands are present by
    a. Taking samples for speciation measurement by voltammetry
    b. Extracting ligands using SPE filters to identify and quantify Fe binding ligands

3. Quantifying all metals in the bioassay experiments during the course of the bio-assay experiment, in order to link responses of phytoplankton to Fe to the actual concentrations of DFe and the other bio-active metals.
    a. DFe shipboard
    b. All metals (incl. Fe) via ICP-MS (shore based)
4. Qualifying and quantifying Fe-binding ligands as well as cobalamin in the bio-assay experiments.
    a. Taking samples for ligand extraction in the shore based lab

Methods and equipment

Sampling. All trace metal CTD and wire casts were sampled for DFe, and major nutrients NO_3/NO_2, PO_4 and Si at all trace metal depths. All filtering (Sartorius®, 0.2µm; Satrobran 300) was done inside the trace metal van under clean conditions. In addition, filtered and unfiltered samples from selected stations were acidified and stored to determine both dissolved and total dissolvable metal concentrations of the 12 metals listed above (Multi-Element (ME) determination) (Biller and Bruland, 2012; Middag, under revision). All time points and treatments from the bio-assay experiments were sampled for shipboard DFe determination as well as shored based ME determination.

Methods for shipboard DFe measurements. Dissolved iron concentrations were measured directly on board by an automated Flow Injection Analysis method (Klunder et al., 2011). Filtered and acidified (0.024 M HCl) seawater was concentrated on a column containing aminodiacetid acid (IDA) after inline pH adjustment to pH 4 using metal free ammonium acetate buffer. The IDA chelating resin binds only transition metals and not the interfering salts. After washing the column with ultra-pure water, the column is eluted with diluted acid. After mixing with luminol, peroxide and ammonium, the oxidation of luminol with peroxide is catalyzed by iron and a blue light is produced and detected with a photon counter. The amount of iron is calculated using a standard calibration line, where a known amount of iron is added to low iron containing seawater. Using this calibration line a number of counts per nM Fe is obtained. Samples were analyzed in triplicate and standard deviation are given. Concentrations of DFe measured on the NBP1409 cruise ranged from 12 pM up to 8.8 nM with the median at 0.36 nM for the entire dataset. The standard deviation varied between 0% and 21% (the latter being exceptional), but was generally on average 3%. The blank was determined daily by analysing acidified MQ water. The blank values were <0.01 nM and no correction was made for this. The average limit of detection, 0.010±0.006 was defined as 3 times the standard deviation of the SAFe S reference sample (Johnson et al., 2007) that was analysed 4 times during this expedition. A total of 430 samples were analysed from the stations and an additional 102 from the bioassay experiments. At the start of every run an internal reference sample was analysed which was a subsample of a large 4 L sample that was collected at the beginning of the cruise. The average value of this sample was 0.33 nM ±0.013 nM (n=18). Three different SAFe reference samples (S (n=4), D1 (n=7) and D2 (n=5)) where analysed regularly early in the cruise and about every 3rd station later on to conserve these scarce reference samples. Results for these reference samples are in good agreement with the consensus values as published May 2013 (http://www.geotraces.org/science/intercalibration/322-standards-and-reference-materials). During each run a drift standard was analysed to account for any sensitivity changes during a run. This was usually less than 5% and not corrected for, but occasionally larger drift of up to 12% was observed and the results were adjusted accordingly.

Ligand extraction. Samples of 4 L were collected at nine selected station at 6 depths. The 4 L of seawater was passed over an Isolute SPE fitler cartridge in the dark at a flowrate of ~ 4 ml per minute. The filters were activated using methanol (2 ml) that was rinsed of with an 11.2 mM ammonium carbonate solution (3 x 2 ml rinses). After extraction the filter was rinsed with 3 x 2 ml 11.2 mM ammonium carbonate solution and stored at -20°C.

Samples for shore based determination. Samples for dissolved and total dissolvable ME determination were collected from the trace metal CTD and wire casts in 60 ml trace metal clean bottles. A total of 370 filtered and 270 samples were collected for ME determination from the stations, plus an additional 190 filtered samples from the bio-assay experiments.

Samples for $\delta^{18}O$ analyses were collected in 25 ml glass vials and stored at ambient temperature. A total of 381 samples were collected. Samples for $\delta^{234}U$, $\delta^{238}U$ and $\delta^{56}Fe$ were collected at 6 stations at 6 depths and 1 station at 4 depths. These samples were filtered and collected in 10 L collapsible containers and acidified (0.024 M HCl).

Samples for Fe-binding ligands were collected at 5 stations at 6 depths. Two bottles of 0.5 L were filled with filtered seawater at all the sampled depths and stored at -20°C . Additionally, a sample of 1L, 0.5 L and 0.25 l were collected from 2 bio-assay experiments and stored under the same conditions for shore based analysis of Fe-binding ligands and cobalamin. Samples were collected in triplicate at the start of the experiment and in triplicate for each treatment at the selected day (day 4 for exp 3 and day 6 for exp 4). An additional experiment was done for the breakdown of cobalamin under different light treatments in the absence of phytoplankton. An addition of 100 pM cobalamin was made to filtered seawater which was incubated in triplicate for 4 days in both the high and low light incubator before sampling.

Preliminary results

The DFe concentrations in the open ocean were extremely depleted to values well below 0.1 nM. Concentrations increased with depth to about 0.15 nM at 300 m and 0.2 -0.3 nM at 750 m. Towards the continent over the continental shelf much higher concentrations of up to 8.8 nM were observed along the 400, 600 and 700 line. Over the shelf, high concentrations were observed near the surface as well as near the bottom, indicating both as surface source as well as a sedimentary source. Highest concentrations were generally observed closest to the continent along these three northerly LTER grid lines (Fig. 1), all showing a similar trend of low concentrations off shore with increasing concentrations towards the continent.

However, along the two southerly occupied lines 200 and 300, values increase from the open ocean towards the continental slope, but then decreased again over the shelf near the continent. At first glance this matches with the salinity distribution over the shelf, indicating a sea ice or glacial ice melt source for the elevated Fe concentrations (Fig. 2). The $\delta^{18}O$ measurements should elucidate which source is the dominant supplier of Fe, but the very low salinity off shore is indicative of sea ice melt and is not accompanied by elevated Fe concentrations, hinting at a glacial source.

Generally it is assumed that deep winter time mixing replenishes the surface layer with Fe (Tagliabue et al., 2014). However, we found that during our occupation of the transect very early on in the austral summer, the Fe concentrations were much lower than expected and did not show any sign of having been replenished during the past winter (Fig. 3). This indicates that for Fe, a surface source is required to fuel phytoplankton blooms. Most likely the retreating ice provides some Fe, but our preliminary data indicates a significant portion of the Fe comes from the waters over the continental shelf that are affected by glacial input.

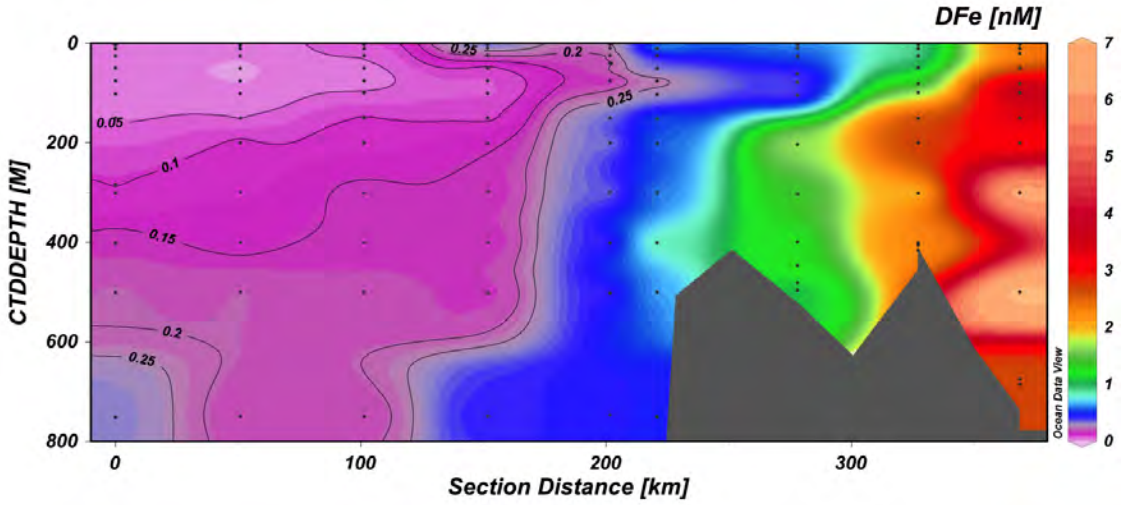

Fig. 1. The DFe distribution along the LTER 600 line going from the open ocean (left), towards the peninsula (right). Note the extremely low concentrations all the way down to 750 m depth and the increasing concentrations towards the continent over the shelf.

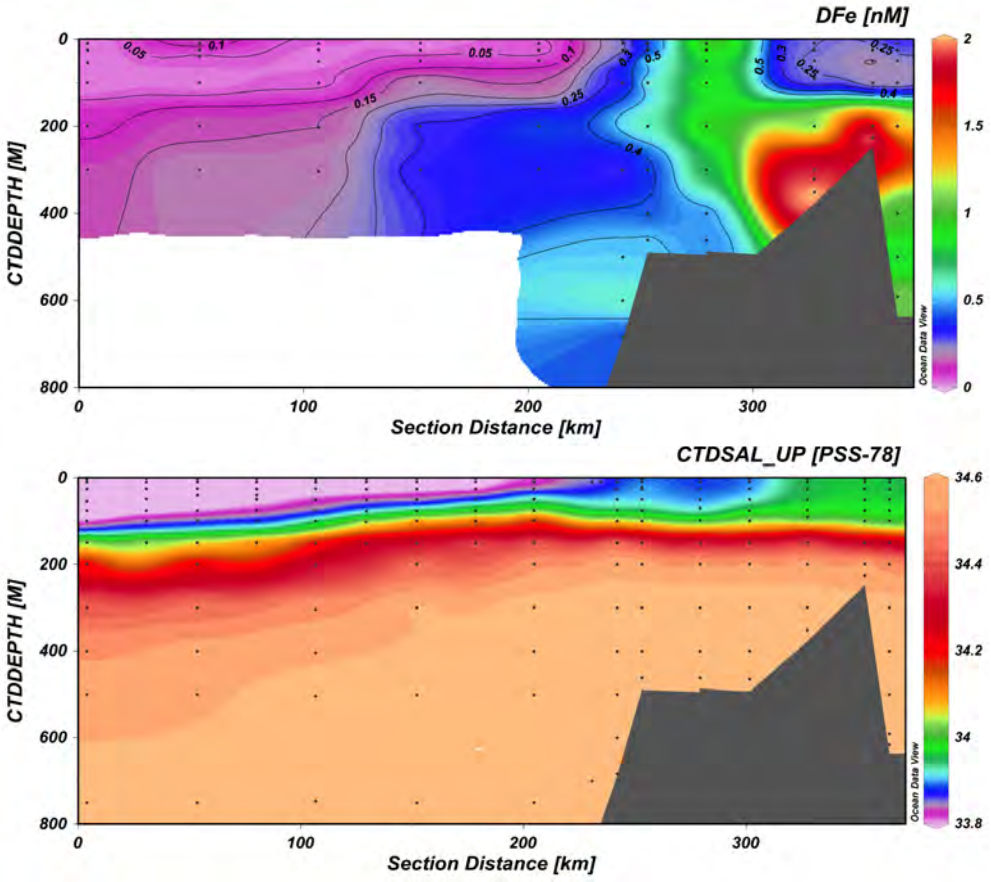

Fig. 2. The DFe distribution (top) and the salinity distribution (bottom) along the LTER 300 line going from the open ocean (left), towards the peninsula (right). Note the elevated DFe along the shelf break that matches with relatively low salinity, whereas off-shore both salinity and DFe are low. Contrasting to the northerly line, relatively low DFe was observed near the continent in the surface, but concentrations were elevated in the deep.

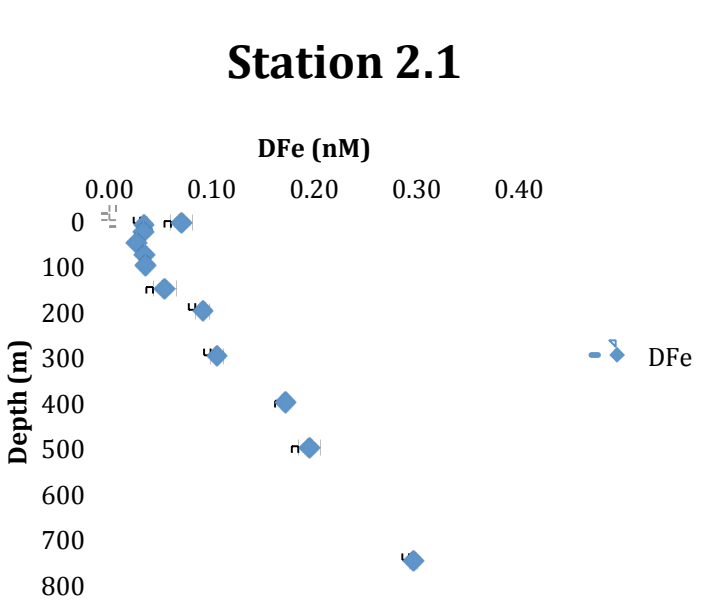

Fig. 3. Vertical profile of DFe concentrations at Station 2.1 of the Western Antarctic Peninsula. Error bars are standard deviations of triplicate measurements.

References

Alderkamp, A.-C. et al., 2012. Iron from melting glaciers fuels phytoplankton blooms in the Amundsen Sea (Southern Ocean): Phytoplankton characteristics and productivity. Deep-Sea Research Part Ii-Topical Studies in Oceanography, 71-76: 32-48.

Arrigo, K.R., Worthen, D.L. and Robinson, D.H., 2003. A coupled ocean-ecosystem model of the Ross Sea: 2. Iron regulation of phytoplankton taxonomic variability and primary production. Journal of Geophysical Research-Oceans, 108(C7).

Bertrand, E.M. et al., 2007. Vitamin B-12 and iron colimitation of phytoplankton growth in the Ross Sea. Limnology and Oceanography, 52(3): 1079-1093.

Biller, D.V. and Bruland, K.W., 2012. Analysis of Mn, Fe, Co, Ni, Cu, Zn, Cd, and Pb in seawater using the Nobias-chelate PA1 resin and magnetic sector inductively coupled plasma mass spectrometry (ICP-MS). Marine Chemistry, 130–131(0): 12-20.

Browning, T.J. et al., 2014. Strong responses of Southern Ocean phytoplankton communities to volcanic ash. Geophysical Research Letters, 41(8): 2014GL059364.

Bruland, K.W., Middag, R., and Lohan, M.C. (Editor), 2014. Controls of Trace Metals in Seawater. Treatise on Geochemistry 2nd edition, 8, 19-55 pp.

Buck, K.N. and Bruland, K.W., 2007. The physicochemical speciation of dissolved iron in the Bering Sea, Alaska. Limnology and Oceanography, 52(5): 1800-1808.

Coale, K.H. et al., 1996. A massive phytoplankton bloom induced by an ecosystem-scale iron fertilization experiment in the equatorial Pacific Ocean. Nature, 383(6600): 495-501.

de Baar, H.J.W. et al., 1990. On iron limitation of the Southern Ocean: experimental observations in the Weddell and Scotia Seas. Marine Ecology Progress Series, 65(2): 105-122.

Gerringa, L.J.A. et al., 2012. Iron from melting glaciers fuels the phytoplankton blooms in Amundsen Sea (Southern Ocean): Iron biogeochemistry. Deep-Sea Research Part Ii-Topical Studies in Oceanography, 71-76: 16-31.

Johnson, K.S. et al., 2007. Developing standards for dissolved iron in seawater. Eos, Transactions American Geophysical Union, 88(11): 131-132.
Klunder, M.B., Laan, P., Middag, R., de Baar, H.J.W. and Bakker, K., 2012. Dissolved iron in the Arctic Ocean: Important role of hydrothermal sources, shelf input and scavenging removal. Journal of Geophysical Research-Oceans, 117.
Klunder, M.B., Laan, P., Middag, R., De Baar, H.J.W. and van Ooijen, J.C., 2011. Dissolved iron in the Southern Ocean (Atlantic sector). Deep-Sea Research Part Ii-Topical Studies in Oceanography, 58(25-26): 2678-2694.
Maldonado, M.T., Strzepek, R.F., Sander, S. and Boyd, P.W., 2005. Acquisition of iron bound to strong organic complexes, with different Fe binding groups and photochemical reactivities, by plankton communities in Fe-limited subantarctic waters. Global Biogeochemical Cycles, 19(4).
Martin, J.H. et al., 1994. Testing the iron hypothesis in ecosystems of the equatorial Pacific Ocean. Nature, 371(6493): 123-129.
Middag, R., Conway, T.M., John, S.G., Bruland, K.W., and de Baar, H.J.W., , under revision. GEOTRACES Intercomparison of Dissolved Trace Elements at the Bermuda Atlantic Time Series Station.
Middag, R., de Baar, H.J.W., Klunder, M.B. and Laan, P., 2013. Fluxes of dissolved aluminum and manganese to the Weddell Sea and indications for manganese co-limitation. Limnology and Oceanography, 58(1): 287-300.
Middag, R., de Baar, H.J.W., Laan, P., Cai, P.H. and van Ooijen, J.C., 2011. Dissolved manganese in the Atlantic sector of the Southern Ocean. Deep-Sea Research Part Ii-Topical Studies in Oceanography, 58(25-26): 2661-2677.
Tagliabue, A. et al., 2014. Surface-water iron supplies in the Southern Ocean sustained by deep winter mixing. Nature Geoscience, 7(4): 314-320.
Thuroczy, C.E. et al., 2012. Key role of organic complexation of iron in sustaining phytoplankton blooms in the Pine Island and Amundsen Polynyas (Southern Ocean). Deep-Sea Research Part Ii-Topical Studies in Oceanography, 71-76: 49-60.
Thuroczy, C.E., Gerringa, L.J.A., Klunder, M.B., Laan, P. and de Baar, H.J.W., 2011. Observation of consistent trends in the organic complexation of dissolved iron in the Atlantic sector of the Southern Ocean. Deep-Sea Research Part Ii-Topical Studies in Oceanography, 58(25-26): 2695-2706.
Velasquez, I. et al., 2011. Detection of hydroxamate siderophores in coastal and Sub-Antarctic waters off the South Eastern Coast of New Zealand. Marine Chemistry, 126(1-4): 97-107.

Genetic characterization of *Phaeocystis antarctica*

Tom O. Delmont, Hilde Oliver, Anton F. Post (not on board), Patricia L. Yager (not on board)

Background

Phaeocystis antarctica is an algal species that often dominates phytoplankton communities in the cold waters of the Southern Ocean. It shows at least two different morphotypes: flagellated free-living unicells and spherical colonies that are thought to be protected from grazing. *P. antarctica* regularly outperforms diatoms and other photosynthetic algae in Antarctic polynyas and (as documented during the Phantastic cruise I), also in the Antarctica Circumpolar Current (ACC) where they form dense phytoplankton blooms and impact the cycles of carbon and sulfur. Yet, little is known on the genetic diversity, metabolic potential and ecological roles of this photosynthetic alga in the Southern Ocean, limiting our ability predicting its acclimation responses to environmental variations. Modern, efficient sequencing technologies provide new opportunities to characterize the genome content of the alga and its associated bacteria, and to assess population diversity in the Southern Ocean. Moreover, it is now possible to deeply sequence phytoplankton bloom transcriptomes, therefore providing critical links between genes expression in *P. antarctica* (especially ones that encode proteins required for environmental stress responses) and key environmental parameters or geochemical activities. Researchers from the Marine Biological Laboratory (Tom Delmont and Anton Post) and Stanford University (Anne-Carlijn Alderkamp and Kevin Arrigo) accomplished a comprehensive functional assessment of the phytoplankton community (mostly diatoms and *P. antarctica*) in the Ross Sea polynya during the 2013-2014 Austral summer bloom event (Phantastic Cruise I). This work further involved the participation of Bethany Jenkins (University of Rhode Island) and Andrew Allen (JCVI). Results indicate a strong response of the phytoplankton community to light and iron availability (Fig. 1).

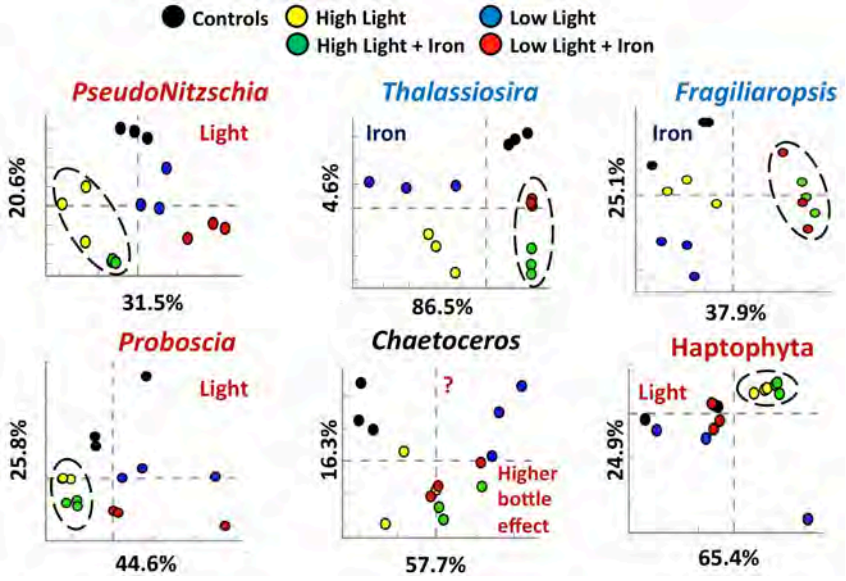

Fig. 1. Principal component analyses based on abundance shift of transcripts determined from the Ross Sea polynya (Phantastic cruise I) when varying environmental parameters (light and iron availability). Sampling was performed after four days of incubation. RNA extraction and sequencing was performed at MBL. Transcripts annotation was performed at JCVI using an in-house pipeline dedicated to the functional and taxonomical annotation of algal transcriptomes.

Moreover, we established that the different algal constituents of the community have distinct functional responses, indicating from a molecular perspective that environmental variations do not impact equally algal taxa in the Southern Ocean. *P. antarctica* was mostly impacted by light, which can be explained by two distinct phenomena: either this alga population was not iron limited (contrasting with several diatom populations occurring in the same community) or it possesses more molecular mechanisms towards the acclimation to light than iron availability. These *in situ* functional investigations are essential to design laboratory experiments and we plan to investigate additional bioassay experiments performed in the Antarctic Peninsula during the Phantastic cruise II.

Objectives

Aim 1. Investigating *P. antarctica* functional activity through gene expression.

Our principal aim was to investigate gene expression within natural populations of *P. antarctica* in coastal waters of the Palmer LTER grid near the Antarctic Peninsula. We first sampled biological material to study the natural functional state of the alga at different depths and locations of this area, including ice samples. Secondly, we sampled the bioassay experiments to investigate transcriptome wide gene expression in natural populations of *P. antarctica* to varying light intensities and iron concentrations. Finally, we collected samples to separately study the functional activity of *P. antarctica* single cells (2-10 µm fraction) and colonies (10-105 µm and >105 µm fractions) using a size fractionation strategy. This fractionation strategy was performed in the water column (low to medium biomass) and in ice samples (high biomass, dominated by *P. antarctica*).

Aim 2: Investigating *P. antarctica* phenotypic and genetic diversity.

The second aim of the project was to investigate the diversity of *P. antarctica* populations in the Southern Ocean. Both phenotypic criteria and genetic markers will be used to observe differences within these populations. For the morphotype investigation, the main objective was to characterize the physical properties of *P. antarctica* colonies (size, number of cells per colony, etc.) on board the vessel using a dissecting microscope. Moreover, samples dedicated to the sequencing of genetic markers (e.g., 16S/18S rRNA gene amplicon datasets) and metagenomes (i.e., all genetic structures present in a given sample) were collected to investigate the genetic diversity of *P. antarctica* in the surface and deeper layers at multiple sites. Finally, the metatranscriptome datasets (see "Aim 1" section) will be used to quantify differentially expressed genes across *P. antarctica* populations, providing additional information regarding their functional diversity.

Aim 3: Investigating bacterial communities associated with *P. antarctica* colonies.

We recently discovered that specialized heterotrophic bacterial taxa associated preferentially with *P. antarctica* colonies in the Amundsen Sea polynya (West Antarctica). The investigation of their genomic content highlighted several functional properties that support both bloom formation and primary productivity of the alga (e.g., cobalamin production). However, additional investigations are required to fully understand these interactions with the alga and their implication for ecosystem biogeochemistry. Therefore, in addition to the genetic investigations of *P. antarctica* natural populations (see "Aim 1" and "Aim 2" sections), our third and last aim during this cruise was to study the diversity and functionality of bacterial communities when associated to (and possibly infecting and/or degrading biomass from) *P. antarctica* colonies in the Antarctic Peninsula. One of the main objectives was to investigate their functional activity when attached to the alga and to define key functional mechanisms directly related to the alga

metabolism.

Methods and sample collection

Throughout sample collection for metatranscriptomic analysis a particular effort was made to collect biological samples in a limited period of time in order to study the *in situ* activity of the alga and prevent changes due to responses to sampling conditions as much as possible.

Phytoplankton sampling for metatranscriptomic datasets (aim 1). Core sampling (44 samples) – Phytoplankton biomass was collected from one to two depths 23 stations. Depending on the biomass, we filtered 0.7-4.0 L onto 0.2 µm filters that were flash frozen in liquid nitrogen and stored at -80°C. Sampling time from collecting samples from the CTD to flash freezing was approximately 25 min.

Bioassay experiments (234 samples) – Five experiments performed by varying light and iron availability (plus B12 vitamin for two experiments) with sampling points at days 4 and 6. Sampling strategy: From each of the treatments phytoplankton biomass was sampled from the triplicate incubation bottles, filtered onto 2 µm filters, flash frozen in liquid nitrogen and stored at -80°C. Sample volume was 0.5 L and less than 15 min was required from sampling to flash freezing.

Size fractionation to disjointedly acquire DNA and RNA from P. antarctica single cells and colonies (aim 1). Phytoplankton biomass was collected in different size fractions of >105 µm (enriched in *P. antarctica* colonies), 2-105µm (enriched in *P. antarctica* single cells, small colonies and diatoms) and <2 µm (enriched in bacteria). In the water column samples were collected at 10 meters depth (36 samples), and in the ice samples were collected at 0-1 meter depth (52 samples).

Sampling for phytoplankton community structure in order to generate 16S/18S rRNA gene amplicons and metagenomic datasets (aim 2). Phytoplankton biomass was collected from surface waters. 0.5 L to 20 L of seawater was filtered onto 0.2 µm filters (41 samples).

Preliminary results: Analysis of *P. antarctica* colonies (aim 2)

Our main activities were focused on sample collection and storage since most of our scientific analyses will be performed at the Marine Biological Laboratory (especially, DNA and RNA extraction, 16S/18S rRNA, metagenomic and metatranscriptomic library constructions, high throughput sequencing, bioinformatics analysis). In addition we made some on-board observations and a few preliminary results are already available. In particular this is the case of microscopy observations on *P. antarctica* colony morphology and abundance.

Station samples. We recorded the density of colonies at distinct water column depths (10 and 50 m) as well as inside the ice where we encountered a substantial *P. antarctica* bloom event (figure 1). We detected about 200 times more colonies per litre in the ice as compared to the euphotic layer in the water column.

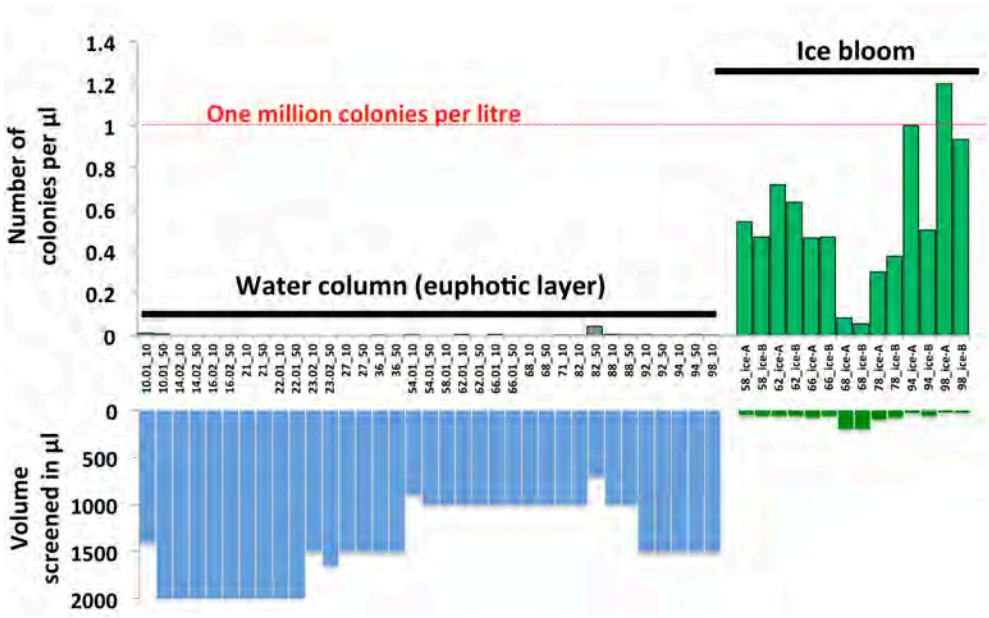

Fig. 1. Number of colonies (and total volume screened to detect them) in the euphotic layer (19 stations, blue bars) and in the ice (7 stations in duplicates, green bars), using samples collected during the Phantastic cruise II and examined with a dissecting microscope.

The ice bloom contained ten times more colonies per litre than what we had encountered in the ACC during the Phantastic cruise I, where about 100 thousands colonies occurred in one litre of water. Based on the density and size of screened colonies, we estimate this *P. antarctica* bloom to occupy ~0.8% of the ice volume, and even up to 3% in station 98. To our knowledge, this is the first quantitative description of a *P. antarctica* bloom inside the ice. The extent of this bloom suggests an important role of ice photosynthetic activity on the overall primary productivity of this section in the Southern Ocean, a component that is largely overlooked in models based on satellite data imaging of open waters.

In addition to colony density, we described their general shape (spherical versus cylindrical) and number of cells per colony (figure 2). Consistent with observations performed during the Phantastic cruise I, only a small fraction of colonies had a spherical shape. At one ice site (station 98), we observed unusually long and thin colonies that might reflect morphological adaptation to the ice environment. However, this morphology was not dominant in other ice stations. Furthermore, the number of cells per colony was similar between the water column and the ice, averaging a score of 100. Overall (and with the exception of station 98), only the density of colonies varied significantly between the water column and the ice. However, it is likely that metabolic activities differ between these two habitats. We acquired samples for metatranscriptomic analysis of colonies occurring in the water column and the ice to investigate these differences.

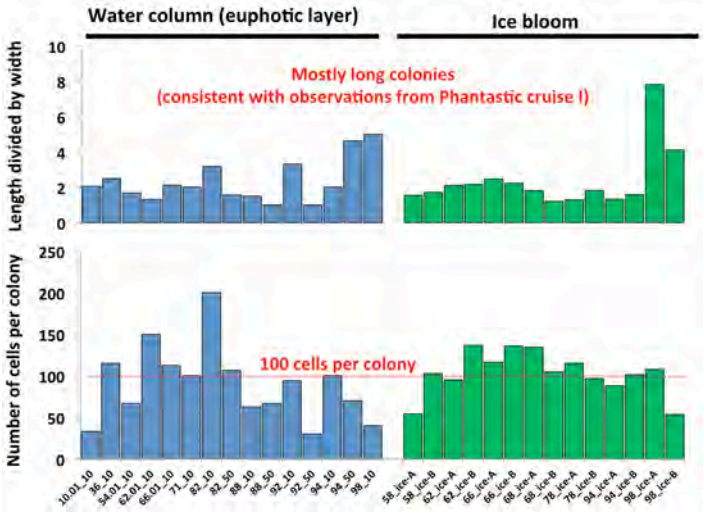

Fig. 2. shape of colonies (length divided by width) and number of cells per colony in the euphotic layer of multiple stations (blue bars) and in the ice (green bars), using samples collected during the Phantastic cruise II and examined with a dissecting microscope.

Bioassay experiments. In addition, we recorded the density and shape of colonies in four out of five Bioassay experiments performed during the Phantastic cruise II. The density of colonies varied substantially between experiments, reflecting high (experiments 2 and 3) and low biomass stations (experiments 4 and 5). We observed a light effect in all conditions and an iron effect in experiments 3 and 5 only.

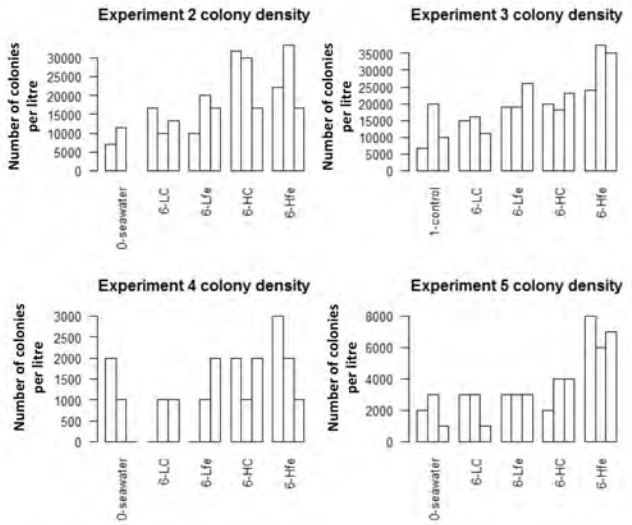

Fig. 3. Number of colonies detected in the Bioassay experiments 2, 3, 4 and 5 (Phantastic cruise II, incubation day 6) as a function of the light and iron availability. Bars represent replicate bottles processed for each condition. For each bottle, colonies were screened of 5-10 drops of 0.1-0.2 millilitres each using a dissecting microscope.

Iron, manganese, Vitamin B12, and light availability to phytoplankton – Bioassay experiments

Anne-Carlijn Alderkamp, Rob Middag, Ella Patterson, Tom Delmont, Erin Bertrand, Gert van Dijken, Erin Dillon, John Butterfield, Anton Post (not on board), Kevin Arrigo

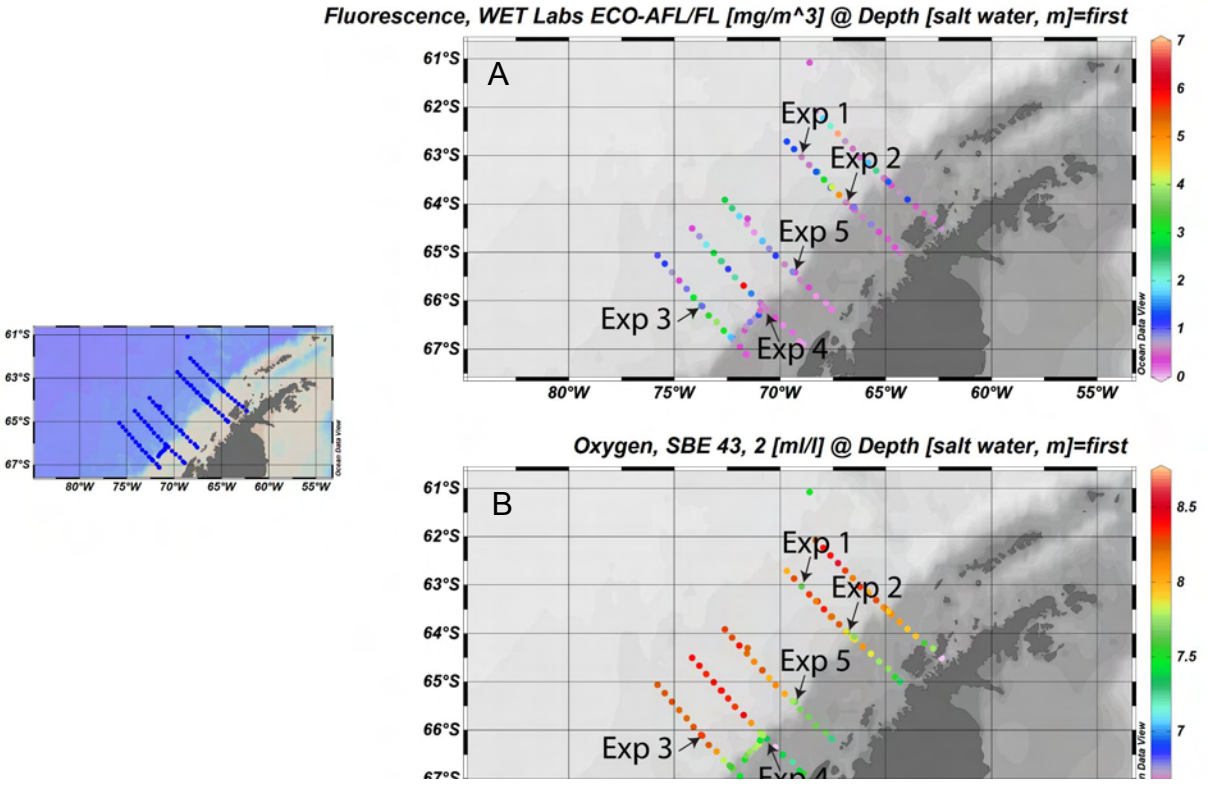

Fig. 1 Location of bioassay experiments and (A) surface fluorescence (arbitrary units) and (B) surface O_2 concentrations (ml L^{-1}).

The interactive effects of the availability of iron (Fe), manganese (Mn), cobalamin (Vit B12), and light on phytoplankton photosynthesis rates and characteristics, biochemical composition, and gene expression were investigated in bioassay experiments. Using the trace metal clean rosette and CTD system, surface water (10-25 m) was obtained at five stations (Fig 1, Table 1) and phytoplankton was incubated in acid washed 2 L polycarbonate bottles under high light (HL; 30% incident irradiance) and low light (LL; 3-5% incident irradiance) at *in situ* water temperature in deck incubators. Fe, Mn, and Vit B12 were added to some treatments that were compared to unamended control treatments. All treatments were tested in triplicate incubations. Trace metal clean techniques were used throughout the experiments and sampling. At day 4 and 6, bottles were taken out and the entire volume was subsampled for a suite of parameters (see table 2). Mn was only tested in experiment 3 and was sampled at day 5. All parameters were also measured in triplicate initial samples.

Table 1. Initial experimental conditions.

Exp	St	Lat (°S)	Long (°W)	Depth (m)	SSS	SST (°C)	SS Fluor	SS pCO_2	Chl a (µg L^{-1})	F_v/F_m	σ	DFe (nM)
1	4	63.04	68.99	10	33.76	-1.56	1.08	303.9	0.40 ±0.01	0.57 ±0.01	741 ±13	0.15 ±0.12
2	10	63.96	66.84	10	33.84	-1.71	4.72	292.3	1.88 ±0.06	0.49 ±0.03	596 ±68	0.10 ±0.01
3	50	66.09	73.75	25	33.69	-1.69	3.53	360.4	1.59 ±0.03	0.54 ±0.01	510 ±23	0.10 ±0.02
4	67	66.19	70.63	25	33.87	-1.77	1.19	431.5	0.64 ±0.02	0.31 ±0.01	496 ±33	0.69 ±0.09
5	78	65.40	69.41	25	33.76	-1.74	1.86	398.8	0.49 ±0.01	0.57 ±0.03	519 ±59	0.04± 0.01

After the loss of the trace metal clean rosette we used a series (approximately 20) of casts with a trace metal clean GoFlo sampler attached to the Kevlar wire to start experiments 3, 4, and 5. Starting experiments in this way took approximately two hours and initial samples were spaced throughout the casts. Because of sampling limitation the Vit B12 treatment was omitted.

Preliminary results

Phytoplankton biomass measured as Chl *a* increased over the incubation time in all treatments in all experiments, showing positive phytoplankton growth rates (Figure 2). The effects of Fe, Mn and Vit B12 additions were tested compared to their control (C) treatments at the same light levels (one-way ANOVA) and effects were considered significant when $p< 0.05$.

We only tested effects of Vit B12 addition in exp 1 and 2. The only effects of Vit B12 were detected in exp 2, where Vit B12 addition resulted in a lower Chl *a* in the LL incubation at T4 and a lower F_v/F_m in the LL incubation at T6 (results not shown). Since there were no effects of Vit B12 addition on Chl *a*, F_v/F_m, or σ_{PSII} in any of the other experiments at either HL or LL (results not shown) we concluded that Vit B12 did not stimulate phytoplankton growth in either experiment and thus we found no indications that vit B12 availability affects phytoplankton growth and productivity in the western Antarctic Peninsula in spring. Similar to Vit B12 additions, we found no effects of Mn additions on Chl *a*, F_v/F_m, or σ_{PSII} in exp 3 at either HL or LL.

Fe-additions affected Chl *a*, F_v/F_m and σ_{PSII} in several experiments, when compared to the control treatments at the same light treatment (Figure 2). Therefore, Fe and light effects on Chl *a*, F_v/F_m and σ_{PSII} were tested in 2-way ANOVAs. Light affected Chl *a* in several incubations (Fig 2), where Chl *a* was generally higher in LL incubations than in HL incubations. Fe-additions stimulated Chl *a* concentrations in LL incubations in several experiments (exp 2, 3, 5), but, surprisingly, Fe-additions resulted in lower Chl a in several HL incubations (exp 2, 3, 4). Thus,

when the effects of Fe on Chl *a* where analyzed with a two-way ANOVA there was no net Fe-effect in most experiments. Exp 5, T6 was the only time point where Chl *a* was higher in the Fe treatments. The opposite effects on HL and LL incubations resulted in an interactive effect of Fe and light in several experiments (Figure 2).

Table 2 Bioassay samples under analysis

Measurement	**Institute**	**Method**	**Exps**
Chl *a* concentration	Stanford	Fluorescence (on board)	all
Variable Fluorescence (F_v/F_m, σ_{PSII})	Stanford	FIRe/PAM (on board)	all
Phytoplankton pigment composition	Stanford/ University of Groningen (Netherlands)	HPLC (institution)	all
Particulate carbon, nitrogen	Stanford	Elemental analyzer (institution)	all
Phytoplankton community composition	Stanford	Flowcam (on board & institution)	all
Photosynthesis vs irradiance characteristics	Stanford	^{14}C incorporation in Photosynthetron (on board)	all
Particle absorption	Stanford	Photospectrometer (on board)	all
Phytoplankton transcriptome analysis	MBL	RNA sequencing (institution)	all
Phytoplankton proteomics	JCVI/Dalhousie University (Canada)	HPLC-MS (institution)	all
Phytoplankton macromolecular composition	Monash University (Australia)	FTIR microspectroscopy and Raman spectroscopy (institution)	all
Nutrients (nitrate, nitrite, phosphate, silicate)	Stanford/ Royal NIOZ (Netherlands)	Autoanalyzer (institution)	all
Dissolved Fe	University of Otago (New Zealand)	Flow Injection Analyzer (on board)	all
Full Dissolved trace metal composition	University of Otago (New Zealand)	ICP-MS (institution)	3, 4
Fe-binding organic ligands	University of Otago (New Zealand)	LC separation and MS/MS detection (institution)	3, 4
Cobalamine (vit B12)	University of Otago (New Zealand)	LC separation and MS/MS detection (institution)	3, 4

Both Fe- and light affected the F_v/F_m of phytoplankton in several experiments (Figure 2). In general, Fe-additions increased F_v/F_m under both LL and HL in all experiments, except in exp. 4, where no Fe-effects were detected. F_v/F_m was higher under LL when compared to HL in all experiments.

Both Fe- and light affected the σ_{PSII} of phytoplankton in several experiments (Figure 2). Fe-additions decreased σ_{PSII} under both LL and HL in exp 1, 2, 3, and 5, although the effect was not always significant at both timepoints. σ_{PSII} was higher in HL incubations than in LL incubations

in exp 2 and 4, but the effect was opposite in exp 3. In general, Fe-effects on σ_{PSII} were larger than light effects (exp 2, 3 and 5).

Overall, we found positive effects of Fe-addition on phytoplankton biomass at LL in several experiments (exp 1, 2, 3, 5). These effects were accompanied by an increase in F_v/F_m, and a decrease in σ_{PSII}. No positive effects of Fe-addition on Chl *a* or F_v/F_m were detected in exp 4, which was located on the continental shelf (Fig 1) and had with initial DFe of 0.69 ±0.09 nM (Table 1), which was at least 4.6 times higher than the initial DFe at other experiments. In all experiments that were located off the continental shelf and on the shelf break (exp 5), Fe-additions stimulated photosynthetic efficiency (measured as F_v/F_m) and in several experiments the Chl *a* concentrations in LL incubations. These experiments suggest phytoplankton off the continental shelf in the western Antarctic Peninsula region may be Fe-limited early in the growing season. These findings are in agreement with the low DFe that was detected throughout surface waters during the NBP 14-09 cruise (see section XX, Rob Middag). Analysis of the physiological, transcriptomics, and proteomics samples listed in Table 2 will provide information on phytoplankton adaptation and acclimation mechanisms to the low Fe availability (see section XX, Tom Delmont and section XX, Erin Bertrand). Moreover, the trace metal measurements (full trace metal composition) will reveal if other trace metals are potentially limiting phytoplankton growth or photosynthesis. Finally, the ligand measurements will reveal if there are any Fe or light effects on ligand production and/or breakdown that may affect Fe-availability to phytoplankton.

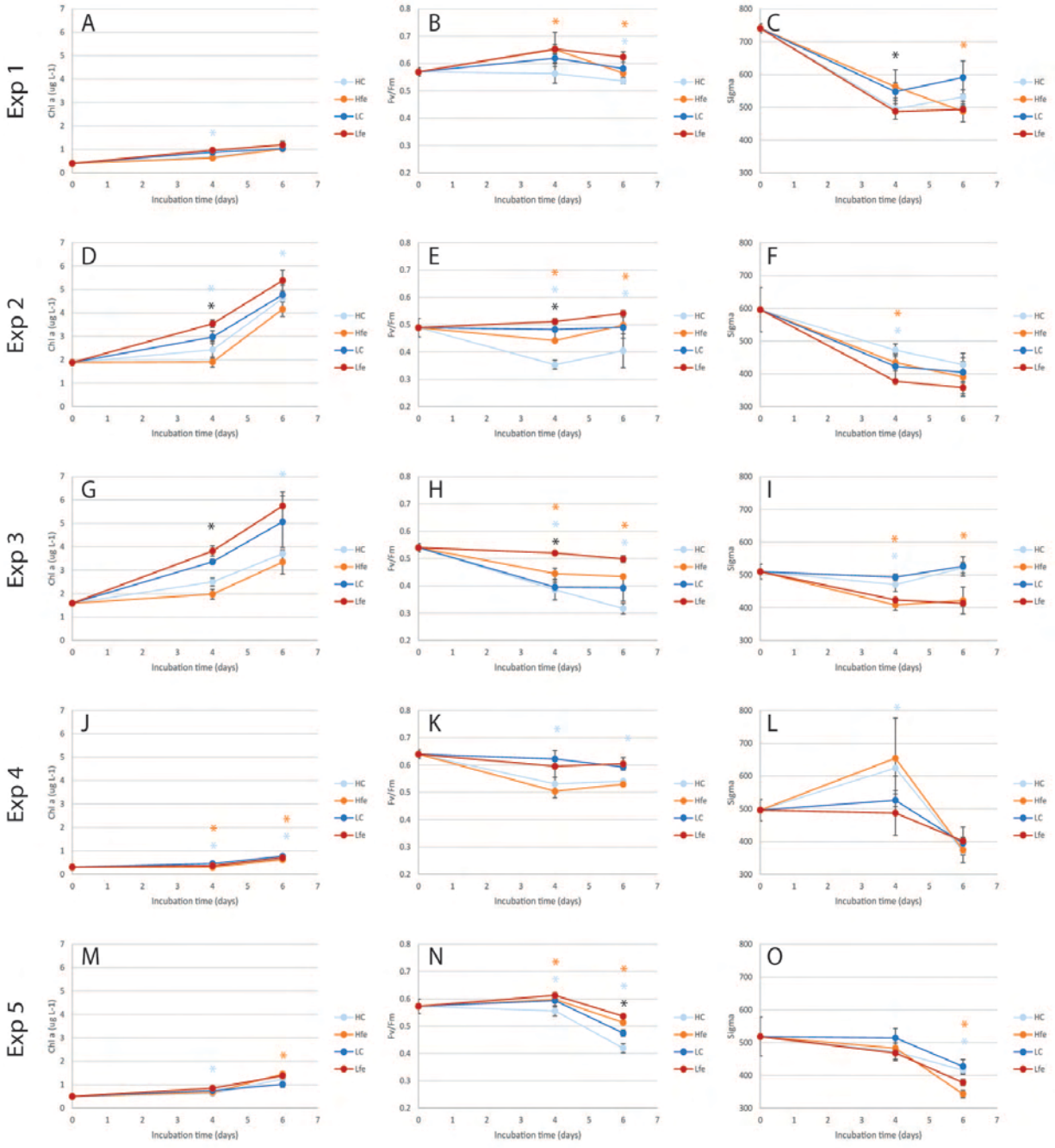

Fig. 2. Responses of Chl *a* (left column), F_v/F_m (middle column) and σ_{PSII} (right column) to Fe-additions in HL and LL incubations in bioassay experiments. Mean and standard deviation of triplicate incubations are shown. * represents significant effects of light, * represents effects of Fe and * represents an interaction between Fe and light effects (two-way ANOVA, p <0.05). HC High light control; HFe High light Fe-addition; LC Low light control, LFe Low light Fe addition.

Proteomics and temperature effects

Erin Bertrand

1. *Proteomic investigations of the influence if iron, light, vitamin B_{12}, and bacterial/archaeal communities on primary producers*

Background and objectives

Proteins are responsible for catalyzing biogeochemical reactions and interfacing between cells and their environment. They also carry, in their amino acid sequences, clues about their phylogenetic source. This makes them potentially excellent tracers of biogeochemical processes. Concentration measurements of specific proteins can be used to estimate rates of processes, to determine which members of a community contribute to those processes, and also what factors, such as nutrient availability, may influence community growth and composition. Bertrand has developed mass-spectrometry based protein measurements for B_{12} biosynthesis in Antarctic marine bacteria and archaea and B_{12} use and starvation in Antarctic diatoms (Bertrand et al 2011, Bertrand et al 2013). These measurements are conducted using HPLC-MS, via isotope dilution selected reaction monitoring mass spectrometry (Figure 1). She will apply these, along with additional peptide measurements currently in development, which will help constrain the role of interactive iron and light limitation in *Phaeocystis* and diatoms as well as interactions between bacterial and phytoplankton communities, to samples obtained during this cruise. This work will be done upon the initiation of her new position at Dalhousie University in July 2015 and will be enabled by collaboration with the Stanford group and the Post Laboratory.

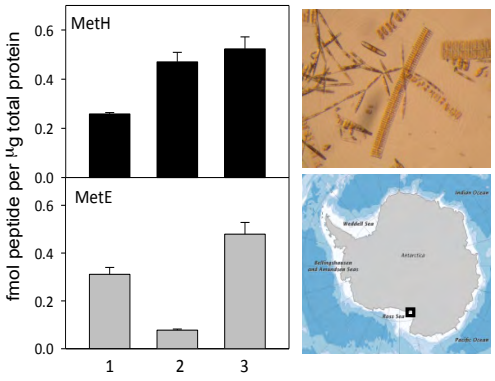

Fig. 1. Concentrations of B_{12}-dependant (MetH) and independent methionine synthase proteins (MetE) in McMurdo Sound diatom communities. These data suggest that there is simultaneous B_{12} use and starvation in Antarctic diatom communities and that peptide measurements are feasible and can yield biogeochemical insights (Bertrand et al 2013).

Sampling achieved:

Daily and main station: Protein samples (6-20 L) were taken from all daily stations and most main stations at two depths (typically 10 m and 50 m) by filtering water obtained from the conventional CTD onto 0.2 micron Sterivex filters via peristaltic pumping. These were preserved at -80C. In total, 72 locations were sampled in duplicate or triplicate.

Ice samples were taken at three ice stations, in two to three discrete locations per station, for both protein and RNA analyses. These samples (30-100 g total weight) were taken by flash freezing ice samples from high biomass locations. Care was taken to protect from light shock during sampling and locations were chosen based on biomass density, selecting those locations that were not exposed to direct irradiance. These samples will be used to assess micronutritional status of phytoplankton, sources of B_{12}, and also differences in gene expression between water column and sea-ice diatoms and *Phaeocystis* in collaboration with the Arrigo, Post, and Allen labs (JCVI).

On-shelf full depth profile: Samples were taken for protein analyses and RNA sequencing (Andrew Allen, JCVI; not on board) from a full depth profile on the shelf (bottom depth 430 m; station 059; 200 line; 12 depths). These will be used to identify potential sources of B_{12} to phytoplankton and to better understand key microbial metabolisms in coastal springtime communities. 8-10 L of seawater were collected per sample, on Sterivex filters as described above, with replicates for protein and RNA analyses.

Bioassay experiments: Protein samples (1.4-2.8 L) were taken from the bioassay experiments 1, 4 and 6 days after the initiation of the experiment. Transcriptome samples were also taken after 1 day, to complement the main transcriptome analyses using a method to analyze short term gene expression changes as a result of changes in micronutrient and light availability. A previous study employing this technique is now in review (Bertrand et al in review; Figure 2).

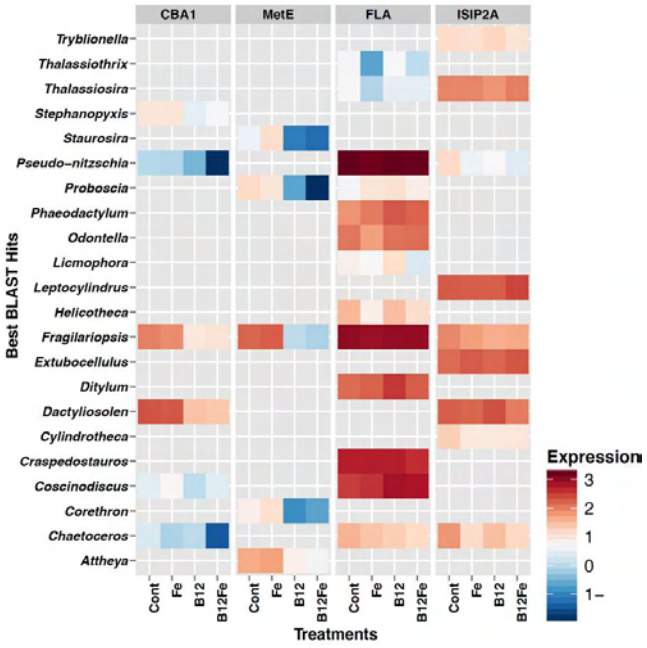

Fig. 2. Heat map displaying the abundance (log10) of transcripts attributed to B_{12} starvation (CBA1, MetE) and iron starvation (FLA and ISIP2A) indicator genes in diatoms 24 h after micronutrient additions to a diatom- dominated community in McMurdo Sound. Transcript abundance is shown for sequences with best blast hits to reference diatom sequences. These data suggest that the community was simultaneously B_{12} and iron stressed (Bertrand et al in review).

2. Influence of temperature on bacterial- phytoplankton interactions

In a previous field season, the ratio of bacterial to phytoplankton abundance and the degree of B_{12} limitation appeared to change as a function of temperature, with bacterial growth not increasing as fast as phytoplankton growth upon elevation of temperature (Bertrand et al *in prep;* Figure 3).

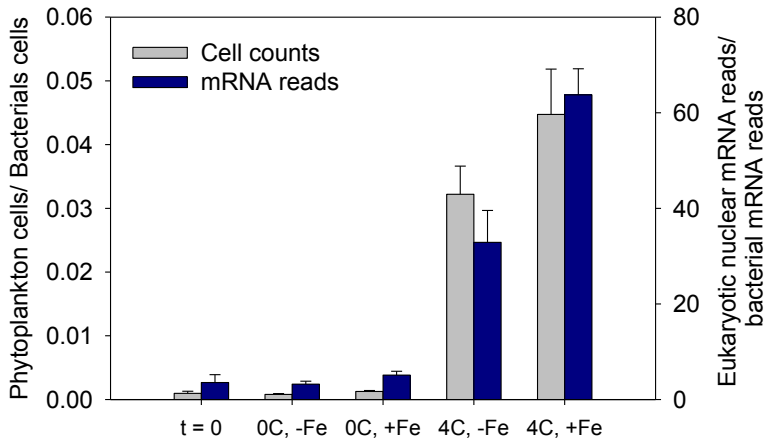

Figure 3: In a bottle incubation experiment started in McMurdo Sound in Jan 2013, elevated temperature changed the ratio of phytoplankton to bacteria, via two measures, cell counting via microscopy and flow cytometry, and mRNA read attribution via RNA sequencing. Bertrand et al *in prep.*

During this cruise, Bertrand conducted an experiment to examine changes in the physical and metabolic relationships between bacteria and phytoplankton as a function of temperature. At two depths, whole water was used to fill 300 mL polycarbonate bottles which we then amended with 2 nM iron as well as a 5% enrichment of ^{13}C-bicarbonate, and placed at -1°C and +4°C Percival incubators set at 60 µE $m^{-2}s^{-1}$. All treatments were prepared in triplicate. After four days, samples were taken for chlorophyll concentrations, phytoplankton cell counts, and bacterial cell counts. Chlorophyll results are shown in Figure 4. The remaining volume was very gently concentrated on a 10 µm filter, resuspended in a small volume, and embedded in a polymer matrix (Technovit) for subsequent analysis via mass spectrometry and microscopy. Samples will be analyzed at Dalhousie University.

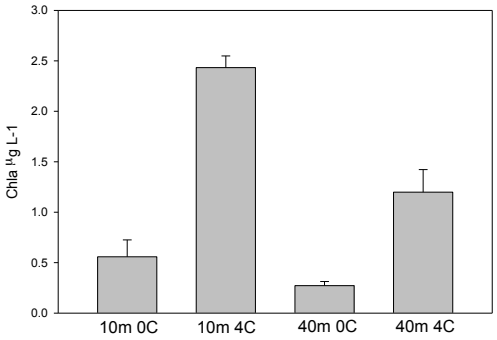

Figure 4: Results from a bottle incubation experiment started on Phantastic II at station 84; elevated temperature increased chlorophyll production after four days. Cell counts, microscopy, and mass spectrometry will provide additional insight into changes in phytoplankton-bacterial dynamics as a function of temperature.

References

Bertrand, E. M, M. A. Saito, Y. J. Jeon, B. A Neilan, Profiling vitamin B_{12} biosynthesis gene diversity in the Ross Sea: the identification of a new group of putative polar B_{12}-biosynthesizers. *Environ Microbiol.* **13**, 1285-1298. (2011).

Bertrand, E. M, D.M. Moran, M.R. McIlvin, J.M. Hoffman, A.E. Allen, M. A. Saito, Methionine synthase interreplacement in diatom cultures and communities: Implications for the persistence of B_{12} use by eukaryotic phytoplankton. *Limnol. Oceano*. **58**, 1431-1450. (2013).

Filtration of samples for diatom DNA and RNA analysis

Laura Filliger and Bethany Jenkins (not on board)

The Jenkins lab has developed high throughput methods to compare diatom community composition (Chappell et al 2013, Whitney et al 2011) and sensitive molecular markers for diatom iron limitation. One of our major goals in participating in this cruise was to collect samples for genetic analysis of diatom community composition and to develop markers of Fe status in Antarctic diatom species. Samples were collected from the conventional CTD cast at every full daily station in the morning. Additional samples were collected during select afternoon and night main stations when core measurements (nutrients, chlorophyll, etc.) were taken. At each CTD where water was collected, biomass was immediately filtered for DNA and RNA samples using a masterflex peristaltic pump with an rpm of 50-60. Triplicate RNA and DNA samples were filtered at each depth determined for P vs. E curves (two depths per cast). Most samples were size fractionated in order to obtain enough biomass on the filters. To size fractionate the samples, a 3μm 25 mm polyester filter was placed upstream of a 0.2μm 25mm Supor filter and biomass was captured on both. In general, 1-3 L of water was filtered, sufficient biomass for down stream analysis.

Samples were also collected for future work aimed at bacteria that are tightly associated with diatoms. At stations with higher biomass, additional triplicate DNA and RNA samples were filtered using 10μm 25 mm polyester filters. About 1.5L of water was filtered from the same two depths as the size-fractionated samples. Because these samples were taken in conjunction with the size fractionated samples, only high biomass stations are represented. High biomass stations required less water to be filtered, and therefore less time, for the same amount of biomass than low biomass stations. Filtering the water quickly was of the upmost importance as RNA in particular is temperature sensitive. All filters were placed in 1.5mL microtubes and flash frozen in a liquid nitrogen dewar. The samples were later transferred to the vessel's -80°C freezer for storage. In total, 666 RNA and DNA samples were collected.

References

Chappell, P. D., L. Whitney, T. L. Haddock, S. Menden-Deuer, E. G. Roy, M. Wells, and B. D. Jenkins. Thalassiosira spp. Community Compostion Shifts in Response to Chemical and Physical Forcing in the Northeast Pacific Ocean Frontiers in Aquatic Microbiology, 23 September (2013)

Whitney, L.P., Lins, J.J., Hughes, M.P., Wells, M.L., Chappell, P.D., and Jenkins, B.D. Characterization of putative iron responsive genes as species-specific indicators of iron stress in Thalassiosiroid diatoms. Frontiers in Aquatic Microbiology 25 November (2011)

Competition Experiments (Ice Algae vs. Phytoplankton)

Ginny Selz

It has been previously suggested that sea ice algae sometimes provide the initial biomass to "seed" phytoplankton blooms (Lannuzel et al. 2013, Mangoni et al. 2009, Garrison et al. 1985). As an area where primary production is tightly linked to sea ice dynamics (Ducklow 2007, Vernet 2008), the Western Antarctic Peninsula is a prime region to examine how the release of ice algae affects the water column. To address these questions, three experiments were completed to study how the plankton communities from the sea ice and water column compete under a variety of conditions (Table 1). Additionally, these competition experiments coupled with settling column experiments gave insight into the sinking rates of phytoplankton originating from the water column (n=6) versus the sea ice (n=8). Together results from these experiments will yield information on the potential ways sea ice algae affect phytoplankton blooms later in the season.

Table 1. Experiment 1 was comprised of 6 treatments: Ice Algae (IA) only, Ice Algae + Water Column Phytoplankton (IAWC), and Water Column Phytoplankton only (WC) under two different light levels: High Light (HL) and Low Light (LL). Experiments 2 and 3 included treatments in 1 as well 3 additional treatments: 90:10 IA:WC HL, 50:50 <20µm IA:WC HL, and 90:10 <20µm IA:WC HL.

	Treatments	**Motivation**
IA (HL/LL)	Ice Algae (IA)	*Ice algae only, response to two different light levels-HL-High Light and LL-Low Light, control for IAWC*
IAWC (HL/LL)	50:50 IA + Water Column (WC) Phytoplankton	*If both communities begin at similar concentrations, who "wins", how does this affect nutrient and element ratios?*
WC (HL/LL)	WC Phytoplankton	*Water column phytoplankton only, response to two different light levels, control for IAWC*
90:10 IAWC (HL)	90:10 IA + WC	*If ice algae are released from the ice at a higher concentration relative to the water column, does this yield the same result as the 50/50 treatment?*
50:50 <20µm (HL)	50:50 <20 µm IA+ <20 µm WC	*If the larger ice algal cells sink out quickly, how does the <20 µm affect the WC composition?*
90:10 <20µm (HL)	90:10 <20µm IA + <20 µm WC	*If <20 µm ice algae are released from the ice at a higher concentration relative to the water column, does this yield the same result as the <20 µm 50/50 treatment?*

Methods

Competition Experiments

Slush layers (ice algae) were collected at ice stations then melted onboard while water was sampled from 10-25m depth at corresponding CTD stations (phytoplankton). Melted slush, whole seawater, and the <20µm fractions were divided into 9 treatments (n=3) based on their chlorophyll a concentrations, determined by in vivo fluorescence. Treatments were incubated in a temperature controlled van onboard under two light levels to simulate a deep (LL) and shallow mixed layer (HL). Treatments were run in triplicate and sampled on day zero (T_0), day four (T_4), and day six (T_6) for pigments (HPLC, Chl *a*), particulate organic carbon and nitrogen(POC/N),

inorganic nutrients (NH_4, NO_3, PO_4, Si), photophysiology (PvE curves, Ap, F0, Fv/Fm, Sigma, and Tau), community composition (FlowCam), and growth rate (^{13}C addition only on T_6).

Settling Column Experiments

Experiment water was collected either from water column stations (10-25m) or from the slush layers during ice stations. Because the biomass was high in the ice layers, slush was first melted and then diluted with FSW to obtain a lower concentration. Whole seawater or melted slush was added to settling columns (n=2,3) following the SetCol protocol (Bienfang, 1981). Columns were incubated in a temperature and light controlled van onboard. Sample water settled for four to twenty four hours and triplicate columns were sampled either all at once or at times two-four hours apart depending on the station. Samples were collected at a top, middle, and bottom port for chlorophyll *a* and FlowCam analysis. Control and T_0 samples were also analyzed for chlorophyll a to correct for any changes over the varied time of the experiment.

Preliminary Results

Preliminary chlorophyll a results suggest there were differences among ice algae and water column treatments within light levels, as well as differences within a group (IA, WC, IAWC) between light levels. These results will also need to be compared with other analyses (particulate organic carbon, growth rates, PE curves, nutrient drawdown) for a more robust conclusion. Settling rates varied were similar among water column stations, but were more varied among ice stations. Settling rates for ice stations (0.25m d^{-1} +/- 0.22) were generally higher than settling rates for water column stations (0.05m d^{-1} +/- 0.04). FlowCam analysis will identify whether certain phytoplankton groups were driving higher ice settling rates.

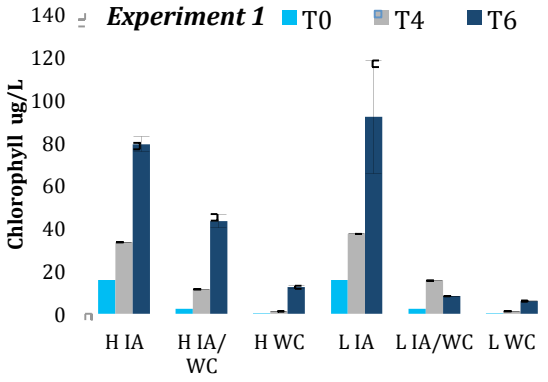

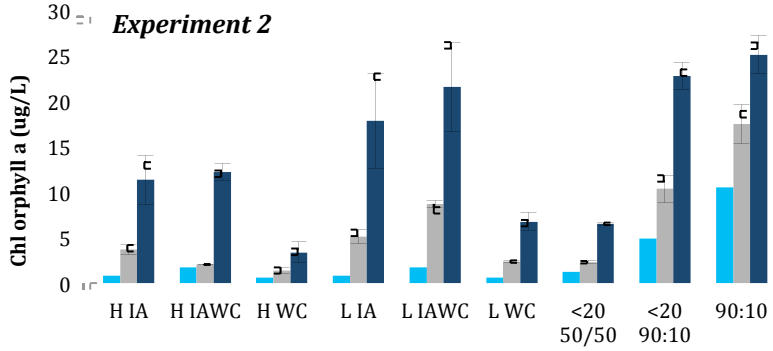

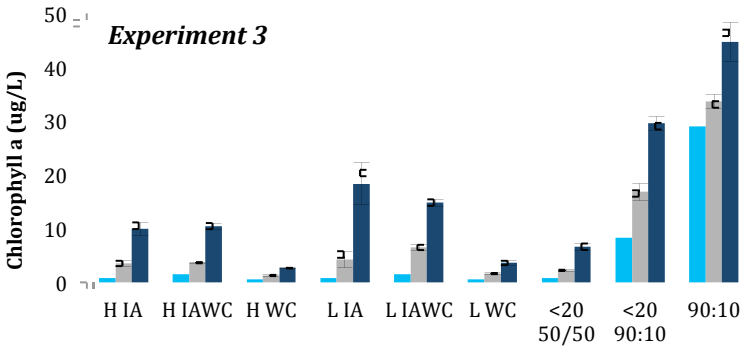

Fig. 1. Chlorophyll *a* for time points T0, T4, and T6 (+/- standard deviation, n=3).